TCR signaling via NFATc1 constrains IL-15-induced NK-like activation of human memory CD8$^+$ T cells

Hoyoung Lee[1,2,4], So-Young Kim[1,4], Sang-Hoon Kim[1,2], Hosun Yu[1], Seongju Jeong[1], Kyung Hwan Kim[1], Chang Gon Kim[1], June-Young Koh[1], Hyung-Don Kim[1], Ji Won Han[1], Su-Hyung Park[1,*], Hyuk Soo Eun[3,*], Eui-Cheol Shin[1,2,*]

[1]Graduate School of Medical Science and Engineering, Korea Advanced Institute of Science and Technology (KAIST), Daejeon 34141, Republic of Korea

[2]The Center for Viral Immunology, Korea Virus Research Institute, Institute for Basic Science (IBS), Daejeon 34126, Republic of Korea

[3]Department of Internal Medicine, Chungnam National University School of Medicine, Daejeon 35015, Republic of Korea

[4]These authors contributed equally to this work.

***Correspondence to:**

Eui-Cheol Shin, M.D., Ph.D., Laboratory of Immunology and Infectious Diseases, Graduate School of Medical Science and Engineering, KAIST, 291 Daehak-ro, Yuseong-gu, Daejeon 34141, Republic of Korea; Tel. +82-42-350-4236; Fax. +82-42-350-4240; email: ecshin@kaist.ac.kr

Hyuk Soo Eun, M.D., Ph.D., Department of Internal Medicine, Chungnam National University School of Medicine, Daejeon 35015, Republic of Korea; Tel. +82-42-280-7418; email: hyuksoo@cnu.ac.kr

Su-Hyung Park, Ph.D., Laboratory of Translational Immunology and Vaccinology, Graduate School of Medical Science and Engineering, KAIST, 291 Daehak-ro, Yuseong-gu, Daejeon 34141, Republic of Korea; Tel. +82-42-350-4288; Fax. +82-42-350-4240; email: park3@kaist.ac.kr

Summary

Here we investigated the regulatory mechanisms of TCR-independent bystander activation and NK-like cytotoxicity of human memory $CD8^+$ T cells. We found that TCR signals suppressed characteristic features of IL-15-induced $CD8^+$ T-cell activation, including increased NKG2D expression and upregulation of genes related to NK cytotoxicity and IFN response. Moreover, ionomycin suppressed IL-15-induced bystander activation and NK-like cytotoxicity, indicating that Ca^{2+}-calcineurin signaling is responsible for TCR-mediated suppression of IL-15-induced bystander activation. In detail, NFATc1 suppressed IL-15-induced bystander activation via binding to AP-1 that is necessary for the IL-15-induced upregulation of NK cytotoxicity-related genes. Consistent with these results, calcineurin inhibitors enhanced IL-15-induced NKG2D expression in the presence of TCR signals. Additionally, we defined genes upregulated by IL-15 and downregulated by concurrent TCR signals as an IL-15-induced bystander activation gene set, and found that this gene signature was upregulated in bystander $CD8^+$ T cells from patients with hepatitis A virus infection. This study paves the way for further investigation of bystander $CD8^+$ T-cell activation in various pathological conditions, and its regulation.

Keywords: Bystander activation, IL-15, TCR, calcium, calcineurin pathway

47 **Graphical abstract**

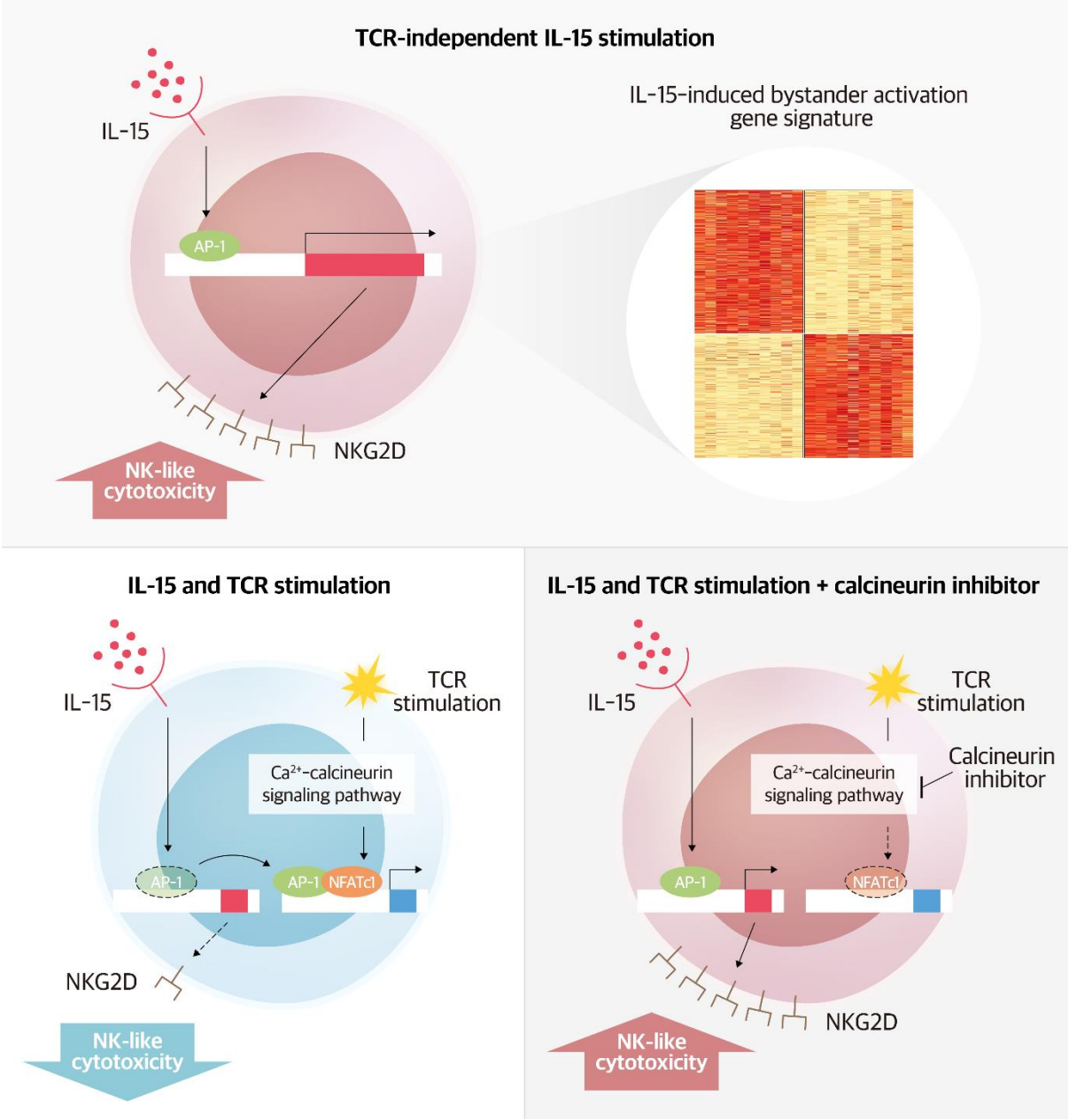

48

Introduction

Memory CD8$^+$ T cells provide prompt and enhanced protection against re-exposures to previously encountered pathogens. These cells are primarily activated by T-cell receptor (TCR) signals, which are triggered by binding to epitope peptides presented by major histocompatibility complex class I (MHC-I)[1] . However, memory CD8$^+$ T cells can also be activated without TCR stimulation by cytokines, a process termed bystander activation[2,3]. Interleukin 15 (IL-15) is reportedly the key driver triggering bystander activation of memory CD8$^+$ T cells[4,5,6,7,8,9,10].

Bystander activation of memory CD8$^+$ T cells can play either protective[6,9,11,12,13,14] or detrimental[8,15,16,17,18] roles in microbial infections, depending on the infecting pathogens. For example, in acute hepatitis A virus (HAV) infection, upregulated IL-15 causes bystander activation of pre-existing memory CD8$^+$ T cells that are specific for HAV-unrelated viruses[8]. These bystander-activated memory CD8$^+$ T cells are characterized by increased expression of the NK-activating receptor NKG2D, together with cytotoxic effector molecules, such as perforin and granzyme B. Consequently, the bystander-activated memory CD8$^+$ T cells recognize and kill target cells via NKG2D-dependent NK-like cytotoxicity, leading to non-specific killing of hepatocytes during acute HAV infection. Notably, this IL-15-induced NK-like cytotoxicity is significantly correlated with liver damage severity in patients with acute HAV infection, indicating the immunopathological role of IL-15-driven bystander-activated memory CD8$^+$ T cells[8].

IL-15-induced bystander-activated memory CD8$^+$ T cells are characterized by upregulated NKG2D and CCR5, which is counteracted by the concurrent TCR stimulation[8,19]. Thus, we can distinguish *bona fide* TCR-independent bystander activation from TCR-mediated conventional activation by examining the expression levels of NKG2D[8] and CCR5[19] on CD8$^+$ T cells. Additionally, studies of a mouse model of bystander activation revealed that IL-15-induced upregulation of IFN-induced transmembrane protein 3 (IFITM3) is also counteracted by concurrent TCR stimulation[20]. These findings indicate that antigen-specific TCR signals restrain cytokine-driven nonspecific activation of memory CD8$^+$ T cells. However, the regulatory mechanisms of IL-15-induced bystander activation of memory CD8$^+$ T cells have not yet been investigated at the molecular level.

In the present study, we investigated specific transcriptional features and regulatory

mechanisms of IL-15-induced bystander $CD8^+$ T-cell activation. We identified a unique set of genes that were upregulated by IL-15 and downregulated by concurrent TCR stimulation. This gene signature, which is related to NK-cell-mediated cytotoxicity and IFN response, was significantly enriched in bystander $CD8^+$ T cells from patients with acute HAV infection. We demonstrated that TCR-induced Ca^{2+}-calcineurin signaling counteracted IL-15-induced bystander activation and NK-like cytotoxic activity. Particularly, NFATc1 suppressed IL-15-induced bystander activation via AP-1 binding. Accordingly, calcineurin inhibitors increased IL-15-induced NKG2D upregulation in the presence of TCR signaling. The current findings reveal a regulatory mechanism of bystander $CD8^+$ T-cell activation, and provide a bystander activation-specific gene signature that will be useful for further investigations of bystander $CD8^+$ T-cell activation in various human diseases.

Results

TCR stimulation counteracts IL-15-induced NKG2D upregulation on memory CD8$^+$ T cells

We analyzed the expression of NKG2D, a marker that is upregulated upon bystander activation[8], on human CD8$^+$ T cells following ex vivo stimulation of healthy donor peripheral blood mononuclear cells (PBMCs) with common gamma chain cytokines, including IL-2, IL-4, IL-7, IL-9, IL-15, and IL-21. The NKG2D expression on CCR7$^-$ memory CD8$^+$ T cells was increased by IL-2, but was more significantly upregulated by IL-15 (**Figure 1A**). On the other hand, any of the tested cytokines did not increase NKG2D expression in naïve CD8$^+$ T cells (**Figure S1**). This IL-15-mediated increase in NKG2D expression on memory CD8$^+$ T cells was dose-dependent, and the effect was saturated at 10 ng/ml (**Figure 1B**).

Next, we examined how TCR stimulation affected NKG2D expression on memory CD8$^+$ T cells. From healthy donor PBMCs, we sorted CCR7$^-$ memory CD8$^+$ T cells to a purity above 99% (**Figure S2**). Following treatment with IL-15, anti-CD3, or both, the NKG2D expression on memory CD8$^+$ T cells was significantly upregulated by IL-15 but not by anti-CD3, and was rather restrained by concurrent anti-CD3 stimulation (**Figure 1C**), confirming our previous findings[8].

On the other hand, memory CD8$^+$ T-cell activation—as indicated by increased co-expression of CD38 and HLA-DR—was synergistically increased by co-stimulation with IL-15 and anti-CD3, compared to by their individual treatment (**Figure 1D**). Upon co-treatment with IL-15 and anti-CD3, memory CD8$^+$ T cells also exhibited synergized increases of Ki-67 expression (**Figure 1E**) and actual proliferation (**Figure 1F**). Taken together, our results demonstrated that TCR and IL-15 synergistically activate memory CD8$^+$ T cells while certain aspects of IL-15-induced bystander activation (e.g., NKG2D upregulation) is suppressed by TCR stimulation.

TCR stimulation suppresses the IL-15-induced upregulation of genes associated with NK-cell-mediated cytotoxicity and IFN response in memory CD8$^+$ T cells

To investigate distinct transcriptional signatures induced by IL-15 and TCR stimulation, we performed bulk RNA-seq of sorted memory CD8$^+$ T cells following stimulation with IL-15, anti-CD3, or the combination of both. Principal component analysis (PCA) revealed clear segregation of IL-15-stimulated memory CD8$^+$ T cells from memory CD8$^+$ T cells stimulated

122 with anti-CD3 or the combination of IL-15 and anti-CD3 (**Figure 2A**). This indicated that IL-15-
123 stimulated memory CD8$^+$ T cells exhibited unique transcriptional features compared to the
124 others. We identified upregulated differentially expressed genes (DEGs) (**Figure 2B**) and
125 clustered them according to their upregulation patterns (clusters 1–7) (**Figure 2C and Table**
126 **S1**). Among the 1,401 DEGs upregulated by IL-15 stimulation, 1,037 were additively or
127 synergistically upregulated by IL-15 and anti-CD3 co-stimulation (Cluster 7) indicating
128 additive/synergistic interaction between TCR- and IL-15-induced signals. On the other hand,
129 we found 118 DEGs were upregulated by IL-15 and not further regulated by concurrent anti-
130 CD3 stimulation (Cluster 6), and 214 were upregulated by IL-15 and downregulated by
131 concurrent anti-CD3 stimulation (Cluster 4).
132 We further directly compared data between IL-15 stimulation and IL-15 plus anti-
133 CD3 co-stimulation (**Figure 2D and Table S2**). We identified a gene set that was upregulated
134 by IL-15 and downregulated by concurrent anti-CD3 (designated as the IL-15-specific gene
135 set), and a gene set that was upregulated by IL-15 and anti-CD3 co-stimulation, but not by IL-
136 15 alone (designated as the TCR-specific gene set). The IL-15-specific gene set included IFN-
137 responsive genes (*IFITM1*, *IFITM2*, *IFITM3*, *PIM1* and *SAMHD1*) and genes associated with
138 NK-cell-mediated cytotoxicity (*KLRK1*, *HCST*, *NCR3*, *GZMA and CD244*). The TCR-specific gene
139 set included genes upregulated by TCR stimulation (*IL2RA*, *IFNG*, *NR4A1*, *NR4A2*, *NR4A3*,
140 *IRF4*, *BATF, MYC*, and *FOS*). Pathway analysis confirmed that the IL-15-specific gene set was
141 significantly enriched with genes related to IFN response and NK-cell-mediated cytotoxicity
142 (**Figure 2E**), and that the TCR-specific gene set was significantly enriched with genes
143 associated with calcineurin-regulated NFAT-dependent transcription, MYC pathway, and cell
144 cycle (**Figure 2F**). Gene set enrichment analysis also demonstrated that the IL-15-specific
145 gene set was significantly enriched with genes associated with the IFN-mediated signaling
146 pathway (**Figure 2G**) and NK-cell-mediated cytotoxicity (**Figure 2H**). Importantly, the IL-15-
147 specific gene set included genes for NKG2D (*KLRK1*), CCR5 (*CCR5*), and IFITM3 (*IFITM3*),
148 which were all previously reported to be upregulated by IL-15, but downregulated by
149 concurrent TCR stimulation in memory CD8$^+$ T cells[8,19,20].
150
151 **Ca^{2+}-mediated signaling suppresses characteristic features of IL-15-induced bystander CD8$^+$**
152 **T-cell activation**

153 We further examined why TCR stimulation suppresses characteristic features of IL-15-
154 induced bystander $CD8^+$ T-cell activation, including the upregulation of genes associated
155 with NK-cell-mediated cytotoxicity and IFN response. We hypothesized that the Ca^{2+}-
156 calcineurin signaling pathway might be responsible for this unique phenomenon, because
157 this pathway is activated by TCR stimulation[21], but not by IL-15 stimulation. We first
158 confirmed that the calcineurin inhibitor FK506 abrogated the TCR-induced activation and
159 proliferation of memory $CD8^+$ T cells (**Figure S3A**), but not IL-15-induced activation and
160 proliferation (**Figure S3B**). On the other hand, the mTOR inhibitor everolimus abolished both
161 TCR- and IL-15-induced activation and proliferation. Consistent with these findings,
162 treatment with another type of calcineurin inhibitor, cyclosporin A (CsA), significantly
163 abrogated the TCR-induced activation and proliferation of memory $CD8^+$ T cells (**Figure S3C**)
164 but did not observably affect IL-15-induced activation and proliferation (**Figure S3D**).
165 To investigate how the Ca^{2+}-calcineurin signaling pathway influenced IL-15-induced
166 bystander $CD8^+$ T-cell activation, we used the Ca^{2+} ionophore ionomycin[22]. Sorted human
167 memory $CD8^+$ T cells were treated with IL-15, ionomycin, or a combination of both, and then
168 subjected to bulk RNA-seq. PCA revealed clear segregation of IL-15-stimulated memory $CD8^+$
169 T cells from the memory $CD8^+$ T cells stimulated with ionomycin or a combination of IL-15
170 plus ionomycin (**Figure 3A**). We identified upregulated DEGs (**Figure 3B**) and clustered them
171 according to their upregulation patterns, from cluster 1 to 7 (**Figure 3C and Table S3**). Like
172 TCR co-stimulation, concurrent ionomycin co-stimulation downregulated a subset of DEGs
173 that were upregulated by IL-15 stimulation (cluster 4). We directly compared IL-15
174 stimulation and co-stimulation with IL-15 plus ionomycin. This led to identification of a gene
175 set that was upregulated by IL-15 and downregulated by concurrent ionomycin treatment
176 (**Figure 3D and Table S4**), which was significantly enriched with genes related to IFN
177 response and NK-cell-mediated cytotoxicity (**Figure 3E**).
178
179 **Ca^{2+}-mediated signaling suppresses IL-15-induced NK-like cytotoxic activity of memory**
180 **$CD8^+$ T cells**
181 We examined the effects of Ca^{2+}-mediated signals on the IL-15-induced NK-like cytotoxic
182 activity of memory $CD8^+$ T cells, which is mediated by IL-15-induced upregulation of NKG2D[8].
183 First, we analyzed NKG2D expression on sorted memory $CD8^+$ T cells from healthy donors

184 following ex vivo stimulation with IL-15, ionomycin, or the combination of both. In line with
185 how TCR stimulation affected IL-15-induced NKG2D expression, ionomycin inhibited IL-15-
186 induced expression of NKG2D on memory $CD8^+$ T cells (**Figure 4A**). However, such
187 ionomycin-induced inhibition did not affect upregulation of the activation markers CD38 and
188 HLA-DR (**Figure 4B**). These findings indicated that Ca^{2+}-mediated signals counteracted only
189 certain aspects of IL-15-induced bystander $CD8^+$ T-cell activation, including the increased
190 surface expression of NKG2D, and the upregulation of genes associated with NK-cell-
191 mediated cytotoxicity and IFN response. We further examined the effect of calcineurin
192 inhibitors on NKG2D expression. As expected, FK506 did not abrogate IL-15-induced NKG2D
193 upregulation on memory $CD8^+$ T cells (**Figure S4**). However, FK506 increased the NKG2D
194 expression when memory $CD8^+$ T cells were stimulated with IL-15 in the presence of anti-
195 CD3 (**Figure 4C**). This observation was consistent with the results of CsA treatment (**Figure**
196 **S5**). This paradoxical effect of calcineurin inhibitors can be explained by inhibition of the
197 counteracting effect of the Ca^{2+}-calcineurin pathway on IL-15-induced NKG2D upregulation.
198 We extended our analysis to examine $CD8^+$ T cells obtained from patients with acute
199 HAV infection, in which the bystander activation of memory $CD8^+$ T cells is well-exemplified[8].
200 Analyzing the NKG2D expression after one day of ex vivo stimulation with IL-15, with or
201 without ionomycin, revealed that IL-15-induced NKG2D upregulation on memory $CD8^+$ T
202 cells was significantly inhibited by the concurrent ionomycin stimulation (**Figure 4D**). We
203 found the same result when we analyzed HCMV- and EBV-specific MHC-I multimer$^+$$CD8^+$ T
204 cells. The paradoxical effect of FK506 on NKG2D expression was also observed when
205 memory $CD8^+$ T cells from patients with acute HAV infection were treated with IL-15 in the
206 presence of anti-CD3 (**Figure 4E**). Finally, we investigated the effect of ionomycin on IL-15-
207 induced NK-like cytotoxic activity, which is mediated by NKG2D. We sorted $CD8^+$ T cells from
208 PBMCs of patients with acute HAV infection (**Figure S6**), and evaluated the NK-like cytotoxic
209 activity against K562 target cells that lacked MHC-I expression. We found that ionomycin
210 significantly decreased the IL-15-induced NK-like cytotoxic activity of $CD8^+$ T cells from
211 patients with acute HAV infection (**Figure 4F**). Collectively, our findings demonstrated that
212 the IL-15-induced NK-like cytotoxic activity of bystander-activated memory $CD8^+$ T cells was
213 restrained by the Ca^{2+}-calcineurin signaling pathway.
214

215 **NFATc1 suppresses IL-15-induced NKG2D upregulation via AP-1 binding**

216 We further investigated a mechanism how the Ca^{2+}-calcineurin signaling pathway constrains
217 IL-15-induced NK-like activation of memory $CD8^+$ T cells at the transcription factor level.
218 First, we found that SP600125, a JNK inhibitor, abrogated IL-15-induced NKG2D upregulation
219 (**Figure 5A**). In addition, SR11302, an AP-1 inhibitor, also abolished IL-15-induced NKG2D
220 upregulation, indicating that IL-15 upregulates NKG2D expression via AP-1 (**Figure 5B**).
221 Furthermore, we performed siRNA transfection for knocking-down the expression of c-Jun
222 and c-Fos, and IL-15-induced NKG2D upregulation was successfully abrogated by
223 transfection of siRNAs for c-Jun and c-Fos (**Figure 5C**).

224 Next, we hypothesized that IL-15-induced AP-1 cannot upregulate NKG2D when it is
225 bound by NFATc1 activated by the Ca^{2+}-calcineurin signaling pathway in the presence of
226 concurrent TCR stimulation. To validate this hypothesis, we performed transfection with
227 plasmids coding for wild-type NFATc1 as well as T551A mutant NFATc1 that cannot bind to
228 AP-1[23]. NKG2D was upregulated by IL-15 in memory $CD8^+$ T cells transfected with control
229 plasmids, and wild-type NFATc1 transfection abrogated IL-15-induced NKG2D upregulation
230 (**Figure 5D**). Importantly, the NKG2D expression in T551A NFATc1-transfected cells was
231 significantly higher than that in wild-type NFATc1-transfected cells although it was not fully
232 restored to the level in control plasmid-transfected cells. This result supports our hypothesis
233 that TCR-induced NFATc1 suppresses IL-15-induced NKG2D upregulation via binding to AP-1.
234 Finally, we validated our hypothesis by using PMA that activates AP-1 via protein kinase C
235 activation. In this experiment, we used PMA and ionomycin instead of IL-15 and TCR
236 stimulation. As expected, The NKG2D expression on memory $CD8^+$ T cells was significantly
237 upregulated by PMA but not by ionomycin, and was restrained by combined treatment with
238 PMA and ionomycin (**Figure 5E**). Taken together, we conclude that TCR signaling via NFATc1
239 constrains IL-15-induced NK-like activation of memory $CD8^+$ T cells.

240

241 **The gene set of IL-15-induced bystander activation is defined and validated**

242 In Figure 2D, the IL-15-specific gene set was identified from genes upregulated by IL-15 and
243 downregulated by concurrent anti-CD3 stimulation, suggesting that the IL-15-specific gene
244 set can be used to distinguish IL-15-induced bystander activation from TCR-induced
245 conventional activation. We investigated whether the IL-15-specific gene set was actually

246 upregulated in TCR-independently IL-15-activated bystander CD8$^+$ T cells in acute HAV
247 infection, where the bystander activation of memory CD8$^+$ T cells is well-exemplified[8].
248 To this end, we performed scRNA-seq using CD8$^+$ T cells obtained from patients with
249 acute HAV infection or healthy donors. We sorted CD8$^+$ T cells from PBMCs, and stained
250 them with DNA-barcoded MHC-I multimers (dCODE dextramers) to detect CD8$^+$ T cells
251 specific for HAV, human cytomegalovirus (HCMV), Epstein-Barr virus (EBV), and influenza A
252 virus (IAV) (**Figure 6A**). We further sorted dCODE dextramer-positive and -negative cells, and
253 then re-mixed them at a 1:9 ratio. Next, the cells were labeled with CITE-seq antibodies, and
254 scRNA-seq was performed using the Chromium system. In uniform manifold approximation
255 and projection (UMAP) visualization, we successfully detected dCODE$^+$ HAV-specific CD8$^+$ T
256 cells, together with HCMV-, EBV- and IAV-specific CD8$^+$ T cells, which we defined as
257 bystander CD8$^+$ T cells (**Figure 6B**). Compared to those from healthy donors, the bystander
258 CD8$^+$ T cells from patients with acute HAV infection exhibited increased surface protein
259 levels of activation markers including CD38 and HLA-DR, and the genes for cytotoxic
260 molecules *PRF1* and *GZMB* (**Figure 6C**). This confirmed our previous finding[8] that bystander
261 CD8$^+$ T cells are activated during acute HAV infection.
262 Next, we applied the IL-15-specific gene set (which was upregulated by IL-15 and
263 downregulated by concurrent anti-CD3) in bulk RNA-seq to scRNA-seq analysis. The IL-15-
264 specific gene set was significantly enriched in bystander CD8$^+$ T cells compared to HAV-
265 specific CD8$^+$ T cells from patients with acute HAV infection (**Figures 6D and E**). Additionally,
266 we found that the IL-15-specific gene set was significantly enriched in dCODE$^-$
267 effector/memory CD8$^+$ T cell cluster compared to HAV-specific CD8$^+$ T cells from patients
268 with acute HAV infection (**Figure S7**). This indicated that the dCODE$^-$ effector/memory CD8$^+$
269 T-cell population included a considerable proportion of non-HAV-specific bystander cells. On
270 the other hand, the TCR-specific gene set (a gene set that was upregulated by IL-15 and anti-
271 CD3 co-stimulation, but not by IL-15 alone in Figure 2D) was significantly upregulated in
272 HAV-specific CD8$^+$ T cells compared to bystander CD8$^+$ T cells (**Figure 6F**). These findings
273 suggest that the IL-15-specific gene set and TCR-specific gene set will be useful for
274 discriminating between IL-15-induced bystander activation and TCR-induced conventional
275 activation. Activation (**Figure S8A**) and enrichment of IL-15-specific gene set (**Figure S8B**) in
276 bystander CD8$^+$ T cells were significantly inhibited at the convalescent phase. We also

277 analyzed a gene set that was upregulated by IL-15 and downregulated by concurrent
278 ionomycin treatment, and found that it was significantly enriched in bystander $CD8^+$ T cells
279 compared to HAV-specific $CD8^+$ T cells (**Figure 6G**), indicating that genes upregulated by IL-15
280 and counteracted by Ca^{2+} are characteristic features of bystander-activated memory $CD8^+$ T
281 cells during acute HAV infection.
282 Detailed analysis revealed that IFN response-related genes (*IFI44L*, *IFIT3*, *IFITM1*,
283 *IFITM2*, *IFNAR1*, *IFNAR2*, *IFNGR1, PIM1 and SAMHD1*) were significantly enriched in
284 bystander $CD8^+$ T cells compared to HAV-specific $CD8^+$ T cells (**Figure 6H**)**.** Furthermore,
285 surface proteins (**Figure 6I**) and genes (**Figure 6J**) associated with NK-cell-mediated
286 cytotoxicity were also significantly increased on bystander $CD8^+$ T cells compared to HAV-
287 specific $CD8^+$ T cells. We again confirmed the upregulation of NKG2D and CCR5 on bystander
288 $CD8^+$ T cells compared to HAV-specific $CD8^+$ T cells (**Figure 6K**). On the other hand, compared
289 to bystander $CD8^+$ T cells, HAV-specific $CD8^+$ T cells exhibited upregulation of CD38, HLA-DR,
290 PD-1, LAG-3, TIM-3, and CD39, together with *IFNG, PRF1, GZMB,* and *MKI67* (**Figure S9**).
291 We also validated the IL-15-specific gene set in a mouse model of bystander $CD8^+$ T-
292 cell activation, in which OT-1 bystander memory cells are activated by PR8 IAV infection, with
293 or without SIINFEKL co-stimulation[20]. We identified the upregulated DEGs in OT-1 memory
294 cells during PR8 infection, compared to in those cells during PR8 infection and SIINFEKL co-
295 stimulation, and found that the IL-15-specific gene set was significantly enriched among the
296 DEGs from the PR8 mouse model (**Figure S10**). On the other hand, the TCR-specific gene set
297 was significantly enriched among the upregulated DEGs in OT-1 memory cells during PR8
298 infection and SIINFEKL co-stimulation, compared to those cells during PR8 infection without
299 SIINFEKL co-stimulation. These findings demonstrate that the IL-15-specific gene set and
300 TCR-specific gene set are good indicators of IL-15-induced bystander activation and TCR-
301 induced conventional activation, respectively. We further conclude that the IL-15-specific
302 gene set, which was upregulated by IL-15 and counteracted by concurrent TCR stimulation,
303 can be used to identify memory $CD8^+$ T cells that are activated by an IL-15-induced
304 bystander mechanism under various conditions.

305 **Discussion**

306 The characteristic features of IL-15-induced bystander activation—including NK-like
307 cytotoxicity and the upregulation of NKG2D and CCR5—are differentially regulated by IL-15
308 and TCR stimulation in memory $CD8^+$ T cells[2,8,19]. However, the molecular characteristics and
309 regulatory mechanisms governing this phenomenon have not been previously explored.
310 Here, we identified a specific set of genes related to NK-cell-mediated cytotoxicity and IFN
311 response, which was upregulated by IL-15 but restrained by concurrent TCR stimulation in
312 memory $CD8^+$ T cells. Moreover, we used ionomycin to demonstrate that Ca^{2+}-calcineurin
313 signaling restrained characteristic features of IL-15-induced bystander activation and NK-like
314 cytotoxicity. Furthermore, we showed that NFATc1 suppressed IL-15-induced bystander
315 activation via AP-1 binding. Consistent with these results, calcineurin inhibitors increased the
316 IL-15-induced NKG2D upregulation on memory $CD8^+$ T cells in the presence of TCR signals.
317 We further defined the genes that were upregulated by IL-15 and suppressed by concurrent
318 TCR stimulation as the gene set of IL-15-induced bystander activation. This gene signature
319 was significantly enriched in bystander $CD8^+$ T cells from patients with acute HAV infection, a
320 prototype disease of bystander $CD8^+$ T-cell activation.

321 IL-15 is a homeostatic cytokine that plays essential roles in the development,
322 proliferation, and maintenance of memory $CD8^+$ T cells[24,25,26,27,28]. However, accumulating
323 evidence has expanded our understanding of IL-15 from a homeostatic cytokine to a potent
324 inducer of bystander $CD8^+$ T-cell activation[2]. Previous studies have shown that IL-15 itself
325 elicits multiple functions of memory $CD8^+$ T cells, independently of TCR signals, including
326 proliferation, synthesis of effector molecules, and cytotoxicity[29,30,31]. It was later
327 demonstrated that IL-15 can activate bystander $CD8^+$ T cells and enhance their NK-like
328 cytotoxic features that contribute to host tissue damage[8,18]. However, limited information is
329 available regarding the specific transcriptional signatures induced by bystander activation in
330 memory $CD8^+$ T cells, which are distinguished from those induced by TCR stimulation.
331 Notably, the specific transcriptional profile of IL-15-induced bystander activation has not
332 been previously profiled in human memory $CD8^+$ T cells.

333 In the present study, we found a unique set of genes upregulated by IL-15 and
334 downregulated by concurrent TCR stimulation, which were enriched with genes associated
335 with NK-cell-mediated cytotoxicity and IFN response. This finding supports previous reports

336 of NK-like cytotoxic activity of IL-15-activated memory CD8$^+$ T cells[5,8,10,30,32,33]. Moreover, the
337 enrichment of IFN response genes among genes upregulated by IL-15 and downregulated by
338 concurrent TCR stimulation also confirms our previous findings that IFN response genes
339 were enriched in bystander-activated memory CD8$^+$ T cells from a mouse model[20]. The gene
340 set of IL-15-induced bystander activation, which was upregulated by IL-15 and counteracted
341 by concurrent TCR stimulation, can be used to identify memory CD8$^+$ T cells that are
342 activated by an IL-15-induced bystander mechanism under various conditions.
343 To validate the IL-15-induced bystander activation gene set in a human disease
344 setting, we performed a scRNA-seq analysis that incorporated dCODE MHC-I multimers.
345 Using this approach, we analyzed single-cell transcriptomes of HAV-specific and bystander
346 (HCMV-, EBV-, and IAV-specific) CD8$^+$ T cells from PBMCs of patients with acute HAV
347 infection. Importantly, the IL-15-induced bystander activation gene set that was upregulated
348 by TCR-independent IL-15 stimulation was significantly enriched in bystander CD8$^+$ T cells
349 from these patients. However, this enrichment was not observed in HAV-specific CD8$^+$ T cells
350 during acute HAV infection. This finding demonstrates that gene set will be useful for
351 distinguishing IL-15-induced bystander CD8$^+$ T-cell activation from TCR-mediated
352 conventional activation. This validated IL-15-induced bystander activation gene set provides
353 a compelling opportunity to explore its use in various other diseases with elevated IL-15
354 levels that correlate with disease severity, in which the phenomenon of TCR-independent
355 CD8$^+$ T-cell activation is implicated[2,34]. For example, the IL-15-induced bystander activation
356 gene set could be used to study alopecia areata[33], in which virtual memory CD8$^+$ T cells
357 activated by IL-15 exert NKG2D-dependent NK-like cytotoxicity. Identifying and analyzing
358 TCR-independent bystander CD8$^+$ T-cell activation in other diseases could enhance our
359 understanding of the roles of bystander-activated CD8$^+$ T cells, elucidating their potential
360 contribution to shaping disease outcomes. Moreover, future research could uncover
361 potential therapeutic targets, which could be used to modulate the immunopathological role
362 of TCR-independent bystander CD8$^+$ T-cell activation in various diseases.
363 Binding of IL-15 to its cellular receptor delivers intracellular signals[35,36], some of
364 which (e.g., mTOR and MAPK signaling pathways) overlap with those induced by TCR
365 stimulation[37]. Due to the overlapping components of signaling pathways, previous reports
366 have focused on the role of IL-15 in amplifying TCR signaling, thereby enhancing various TCR-

367 mediated effector functions of $CD8^+$ T cells[38,39,40]. However, the Ca^{2+}-calcineurin signaling
368 pathway discriminates between TCR and IL-15 signals. Upon TCR ligation, Ca^{2+} is released
369 into the cytosol, leading to a rapid influx of extracellular Ca^{2+} until its level is highly
370 sustainable for T-cell activation[41]. The accumulated cytosolic Ca^{2+} binds to calmodulin,
371 leading to a subsequent conformational change in calmodulin for its interaction with the
372 protein phosphatase calcineurin[42]. This interaction dephosphorylates NFATc1, which leads to
373 its translocation into the nucleus, where it binds to AP-1 and regulates various T-cell
374 functions. However, IL-15 stimulation does not activate the Ca^{2+}-calcineurin signaling
375 pathway, as indicated by our present finding that calcineurin inhibitors had no effect on IL-
376 15-induced $CD8^+$ T-cell activation. Instead, Ca^{2+} signals suppress characteristic features of the
377 IL-15-induced bystander activation of memory $CD8^+$ T cells, including upregulation of NKG2D
378 the IL-15-induced bystander activation gene set, and NK-like cytotoxic activity.
379 Calcineurin inhibitors, such as FK506 and CsA, are widely used as
380 immunosuppressants in organ transplantation settings and for the treatment of
381 autoimmune diseases[43]. However, previous studies have reported that calcineurin inhibitors
382 do not affect the cytokine-induced production of IL-17A and IFN-γ from mouse memory-like
383 $CD4^+$ T cells[44]. Consistently, we demonstrated that calcineurin inhibitors failed to suppress
384 the IL-15-induced activation and proliferation of memory $CD8^+$ T cells. Moreover, calcineurin
385 inhibitors paradoxically upregulated the IL-15-induced NKG2D expression on memory $CD8^+$ T
386 cells in the presence of TCR co-stimulation. This suggests that calcineurin inhibitors may
387 enhance NK-like cytotoxic activity of memory $CD8^+$ T cells, and exacerbate $CD8^+$ T cell-
388 mediated immunopathology in IL-15-associated pathological conditions. The data from our
389 current study suggests that immunosuppressive regimens must be carefully selected for the
390 treatment of chronic inflammatory diseases, depending on the mechanism of $CD8^+$ T-cell
391 activation.
392 The recent recognition that bystander activation of memory $CD8^+$ T cells can
393 potentially impact disease outcomes has attracted great attention. Our present study
394 highlights characteristic features and regulatory mechanisms underlying IL-15-induced
395 bystander activation in human memory $CD8^+$ T cells. We demonstrated that IL-15-induced
396 bystander activation exhibits NK-like qualities, rather than being an inherent aspect of the
397 adaptive immune response. Moreover, we found that TCR stimulation plays a role in

398 preventing such antigen-nonspecific NK-like activation through Ca^{2+}-calcineurin-NFATc1
399 signaling, thereby preserving the intrinsic nature of the adaptive immune response.
400 Increasing our understanding of the mechanisms underlying the IL-15-induced bystander
401 activation of memory $CD8^+$ T cells will have important clinical implications for the
402 appropriate treatment of patients whose tissues are damaged by $CD8^+$ T cell-mediated
403 immunopathogenesis.

RESOURCE AVAILABILITY

Lead contact

Further information and requests for resources and reagents should be directed to and will be fulfilled by the lead contact, Eui-Cheol Shin (ecshin@kaist.ac.kr).

Materials availability

The study did not produce novel, distinctive materials or substances.

Data and code availability

All analyzed sequencing data will be available online. Bioinformatic analyses were performed using open-source software and in-house scripts in R (version 4.1.0), which are available from the corresponding author upon reasonable request.

Acknowledgement

This work was supported by the Bio&Medical Technology Development Program of the National Research Foundation (NRF) funded by the Korean government (MSIT) (RS-2024-00439160 and RS-2024-00512914) and by the Institute for Basic Science (IBS), Republic of Korea (IBS-R801-D2).

Author contributions

H.L. and E.C.S. designed the study. H.S.E. collected and provided human clinical samples and information. H.L., S.Y.K., S.H.K., and K.H.K. performed the experiments and collected data. H.L., S.Y.K., S.H.K., H.Y., S.J., K.H.K., C.G.K., J.Y.K., H.D.K., J.W.H., S.H.P., and E.C.S were involved in data analysis and interpretation. H.L., S.Y.K., and H.Y. performed statistical analysis. H.L., S.Y.K., and E.C.S. drafted the manuscript with comments from all authors.

Competing interests

The authors have no conflicts of interest.

INCLUSION AND DIVERSITY

We support inclusive, diverse, and equitable conduct of research.

433 **KEY RESOURCES TABLE**

REAGENT or RESOURCE	SOURCE	IDENTIFIER
Antibodies		
BV510 Anti-human CD3 (clone UCHT1),	BD Biosciences	Cat# 563109 RRID:AB_2732053
BV605 Anti-human CD8 (clone SK1)	BD Biosciences	Cat# 564116 RRID:AB_2869551
BV711 Anti-human Ki-67 (clone B56)	BD Biosciences	Cat# 563755 RRID:AB_2738406
PerCP-Cy5.5 Anti-human CD4 (clone RPA-T4)	BD Biosciences	Cat# 560650 RRID:AB_1727476
AlexaFluor 700 Anti-human CD3 (clone UCHT1)	BD Biosciences	Cat# 557943 RRID:AB_396952
PerCP-Cy5.5 Anti-human CD14 (clone M5E2)	BD Biosciences	Cat# 550787 RRID:AB_393884
PerCP-Cy5.5 Anti-human CD19 (clone H fIB19)	BD Biosciences	Cat# 561295 RRID:AB_10644017
PE Anti-human NKG2D (clone 1D11)	BD Biosciences	Cat# 561815 RRID:AB_10896282
PE-CF594 Anti-human CD14 (clone MPHIP9)	BD Biosciences	Cat# 562335 RRID:AB_11153663
PE-CF594 Anti-human CD19 (clone HIB19)	BD Biosciences	Cat# 562294 RRID:AB_11154408
Pe-Cy7 Anti-human CD45RA (clone HI100)	BD Biosciences	Cat# 560675 RRID:AB_1727498
AlexaFluor 700 Anti-human CD45RA (clone HI100)	BD Biosciences	Cat# 560673 RRID:AB_1727496
APC Anti-human HLA-DR (clone G46-6)	BD Biosciences	Cat# 559866 RRID:AB_398674
BV650 Anti-Human HLA-DR (clone L203)	BD Biosciences	Cat# 752489

		RRID:AB_2917482
AlexaFluor 700 Anti-human CD3 (clone UCHT1)	BD Biosciences	Cat# 557943 RRID:AB_396952
AlexaFluor 700 Anti-human CD38 (clone HIT2)	BD Biosciences	Cat# 560676 RRID:AB_1727472
APC-H7 Anti-human CD8 (clone SK1)	BD Biosciences	Cat# 560273 RRID:AB_1645482
FITC Anti-human CD16 (clone B73.1)	BD Biosciences	Cat# 561308 RRID:AB_10644202
BV421 anti-human NKG2D (clone 1D11)	Biolegend	Cat# 320821 RRID:AB_2566510
PerCP/cy5.5 Anti-human CD197 (CCR7) (clone G043H7)	Biolegend	Cat# 353220 RRID:AB_10916121
APC/Cyanine7 Anti-human HLA-DR (clone L243)	Biolegend	Cat# 307618 RRID:AB_493586
TotalSeq™-C0034 anti-human CD3 Antibody (clone UCHT1)	Biolegend	Cat# 300479 RRID: AB_2800723
TotalSeq™-C0045 anti-human CD4 Antibody (clone SK3)	Biolegend	Cat# 344651 RRID:AB_2800921
TotalSeq™-C0046 anti-human CD8 Antibody (clone SK1)	Biolegend	Cat# 344753 RRID:AB_2800922
TotalSeq™-C0047 anti-human CD56 (NCAM) Antibody (clone 5.1H11)	Biolegend	Cat# 362559 RRID:AB_2801002
TotalSeq™-C0051 anti-human CD14 Antibody (clone 63D3)	Biolegend	Cat# 367137 RRID:AB_2810576
TotalSeq™-C0063 anti-human CD45RA Antibody (clone HI100)	Biolegend	Cat# 304163 RRID:AB_2800764
TotalSeq™-C0083 anti-human CD16 Antibody (clone 3G8)	Biolegend	Cat# 302065 RRID:AB_2800738
TotalSeq™-C0085 anti-human CD25 Antibody	Biolegend	Cat# 302649

(clone BC96)		RRID: AB_2800745
TotalSeq™-C0087 anti-human CD45RO Antibody (clone UCHL1)	Biolegend	Cat# 304259 RRID: AB_2800766
TotalSeq™-C0088 anti-human CD279 (PD-1) Antibody (clone EH12.2H7)	Biolegend	Cat# 329963 RRID: AB_2800862
TotalSeq™-C0089 anti-human TIGIT (VSTM3) Antibody (clone A15153G)	Biolegend	Cat# 372729 RRID: AB_2801021
TotalSeq™-C0101 anti-human CD335 (NKp46) Antibody (clone 9 E2)	Biolegend	Cat# 331941 RRID: AB_2800874
TotalSeq™-C0138 anti-human CD5 Antibody (clone UCHT2)	Biolegend	Cat# 300637 RRID: AB_2800726
TotalSeq™-C0139 anti-human TCR γ/δ Antibody (clone B1)	Biolegend	Cat# 331231 RRID: AB_2814199
TotalSeq™-C0140 anti-human CD183 (CXCR3) Antibody (clone G025H7)	Biolegend	Cat# 353747 RRID: AB_2800949
TotalSeq™-C0141 anti-human CD195 (CCR5) Antibody (clone J418F1)	Biolegend	Cat# 359137 RRID: AB_2810570
TotalSeq™-C0145 anti-human CD103 (Integrin αE) Antibody (clone BerACT8)	Biolegend	Cat# 350233 RRID: AB_2800933
TotalSeq™-C0146 anti-human CD69 Antibody (clone FN50)	Biolegend	Cat# 310951 RRID: AB_2800810
TotalSeq™-C0147 anti-human CD62L Antibody (clone DREG-56)	Biolegend	Cat# 304851 RRID: AB_2800770
TotalSeq™-C0148 anti-human CD197 (CCR7) Antibody (clone G043H7)	Biolegend	Cat# 353251 RRID: AB_2800943
TotalSeq™-C0149 anti-human CD161 Antibody (clone HP-3G10)	Biolegend	Cat# 339947 RRID: AB_2810532
TotalSeq™-C0151 anti-human CD152 (CTLA-4) Antibody (clone BNI3)	Biolegend	Cat# 369621 RRID: AB_2801015
TotalSeq™-C0152 anti-human CD223 (LAG-3)	Biolegend	Cat# 369335

Antibody (clone 11C3C65)		RRID: AB_2814327
TotalSeq™-C0154 anti-human CD27 Antibody (clone O323)	Biolegend	Cat# 302853 RRID: AB_2800747
TotalSeq™-C0155 anti-human CD107a (LAMP-1) Antibody (clone H4A3)	Biolegend	Cat# 328649 RRID: AB_2800854
TotalSeq™-C0159 anti-human HLA-DR Antibody (clone L243)	Biolegend	Cat# 307663 RRID: AB_2800795
TotalSeq™-C0165 anti-human CD314 (NKG2D) Antibody (clone 1D11)	Biolegend	Cat# 320837 RRID: AB_2800844
TotalSeq™-C0168 anti-human CD57 Recombinant Antibody (clone QA17A04)	Biolegend	Cat# 393321 RRID: AB_2801030
TotalSeq™-C0169 anti-human CD366 (Tim-3) Antibody (clone F38-2E2)	Biolegend	Cat# 345049 RRID: AB_2800925
TotalSeq™-C0170 anti-human CD272 (BTLA) Antibody (clone MIH26)	Biolegend	Cat# 344527 RRID: AB_2800919
TotalSeq™-C0176 anti-human CD39 Antibody (clone A1)	Biolegend	Cat# 328237 RRID: AB_2800853
TotalSeq™-C0179 anti-human CX3CR1 Antibody (clone K0124E1)	Biolegend	Cat# 355705 RRID: AB_2800960
TotalSeq™-C0224 anti-human TCR α/β Antibody (clone IP26)	Biolegend	Cat# 306743 RRID: AB_2800793
TotalSeq™-C0250 anti-mouse/human KLRG1 (MAFA) Antibody (clone 2F1/KLRG1)	Biolegend	Cat# 138433 RRID: AB_2800649
TotalSeq™-C0355 anti-human CD137 (4-1BB) Antibody (clone 4B4-1)	Biolegend	Cat# 309839 RRID: AB_2800807
TotalSeq™-C0368 anti-human CD226 (DNAM-1) Antibody (clone 11A8)	Biolegend	Cat# 338337 RRID: AB_2800899
TotalSeq™-C0386 anti-human CD28 Antibody (clone CD28.2)	Biolegend	Cat# 302963 RRID: AB_2800751
TotalSeq™-C0389 anti-human CD38 Antibody	Biolegend	Cat# 303543

(clone HIT2)		RRID: AB_2800758
TotalSeq™-C0390 anti-human CD127 (IL-7Rα) Antibody (clone A019D5)	Biolegend	Cat# 351356 RRID: AB_2800937
TotalSeq™-C0420 anti-human CD158 (KIR2DL1/S1/S3/S5) Antibody (clone HP-MA4)	Biolegend	Cat# 339517 RRID: AB_2814252
TotalSeq™-C0581 anti-human TCR Vα7.2 Antibody (clone 3C10)	Biolegend	Cat# 351735 RRID: AB_2810556
TotalSeq™-C0584 anti-human TCR Vα24-Jα18 (iNKT cell) Antibody (clone 6B11)	Biolegend	Cat# 342925 RRID: AB_2810529
TotalSeq™-C0592 anti-human CD158b (KIR2DL2/L3, NKAT2) Antibody (clone DX27)	Biolegend	Cat# 312619 RRID: AB_2819944
TotalSeq™-C0599 anti-human CD158e1 (KIR3DL1, NKB1) Antibody (clone DX9)	Biolegend	Cat# 312725 RRID: AB_2814161
TotalSeq™-C0801 anti-human CD337 (NKp30) Antibody (clone P30-15)	Biolegend	Cat# 325219 RRID: AB_2800851
TotalSeq™-C0802 anti-human CD336 (NKp44) Antibody (clone P44-8)	Biolegend	Cat# 325119 RRID: AB_2810484
TotalSeq™-C0804 anti-human CD186 (CXCR6) Antibody (clone K041E5)	Biolegend	Cat# 356023 RRID: AB_2876677
TotalSeq™-C0867 anti-human CD94 Antibody (clone DX22)	Biolegend	Cat# 305523 RRID: AB_2814143
TotalSeq™-C0896 anti-human CD85j (ILT2) Antibody (clone GHI/75)	Biolegend	Cat# 333725 RRID: AB_2814226
TotalSeq™-C1021 anti-human GPR56 Antibody (clone 4C3)	Biolegend	Cat# 391907 RRID: AB_2832737
CD3 monoclonal antibody (clone OKT3) Functional Grade	Invitrogen	Cat# 16-0037-85 RRID: AB_468854
Fluorescein-conjugated Anti-human CCR7 (clone 150503)	R&D Systems	Cat# FAB197F RRID: AB_2259847
Chemicals, Peptides and Recombinant Proteins		

Brilliant Stain Buffer	BD Biosciences	Cat# 563794
7-AAD	BD Biosciences	Cat# 559925
Recombinant human IL-2 protein	Peprotech	Cat# 200-0
Recombinant human IL-4 protein	Peprotech	Cat# 200-04
Recombinant human IL-7 protein	Peprotech	Cat# 200-07
Recombinant human IL-9 protein	Peprotech	Cat# 200-09
Recombinant human IL-15 protein	Peprotech	Cat# 200-15
Recombinant human IL-21 protein	Peprotech	Cat# 200-21
Dimethyl sulfoxide	Sigma-Aldrich	Cat# R8418
Tacrolimus (FK506)	Selleckchem	Cat# S5003
Everolimus (RAD001)	Selleckchem	Cat# S1120
PMA	Sigma-Aldrich	Cat# P1585
Ionomycin calcium salt	Sigma-Aldrich	Cat# I3909
Lymphocyte Separation Medium	Corning	Cat# 25-072-CV
Trizol reagent	Invitrogen	Cat# 15-5960-18
Critical Commercial Assays		
LIVE/DEAD fixable aqua dead cell stain kit	Invitrogen	Cat# L34957
LIVE/DEAD fixable Red dead cell stain kit	Invitrogen	Cat# L34972
Intracellular fixation & permeabilization buffer set	Invitrogen	Cat# 88-8824-00
Neon™ NxT Electroporation System 100-µL Kit	Invitrogen	Cat# N10025
CellTrace Violet Cell Proliferation Kit	Invitrogen	Cat# C34557
Anti-FITC microbeads	Miltenyi Biotec	Cat# 130-048-701
CD8 MicroBeads, human	Miltenyi Biotec	Cat# 130-045-201
Human $CD8^+$ T cell isolation kit	Miltenyi Biotec	Cat# 130-096-495
Recombinant DNA		
pcDNA3.1_empty	Genescript	N/A
pcDNA3.1_NFATc1_WT	Genescript	N/A
pcDNA3.1_NFATc1_T551_MT	Genescript	N/A
siRNAs		
Silencer™ Select Negative Control No. 1 siRNA	Invitrogen	Cat# 4390844

Silencer™ Select c-Fos siRNA	Invitrogen	Cat# 4392420
Silencer™ Select c-Jun siRNA	Invitrogen	Cat# 4392420
Software and Algorithms		
FlowJo (version 10.7.2)	Tree Star	https://www.flowjo.com/solutions/flowjo/downloads
Prism (version 8.4)	GraphPad	http://www.graphpad.com/scientific-software/prism/
R v.4.1.0	The R foundation	N/A
Cell Ranger	R package	Version 3.1.0
Seurat package	R package	Version 3.2.2
STAR aligner	R package	Version 2.5.1b
DESeq2	R package	Version 1.24.0
ComplexHeatmap	R package	Version 2.15.4
Bowtie2	R package	Version 2.2.9
limma	R package	Version 4.3
fgsea	R package	Version 1.22.0
biomaRt	R package	Version 2.50.0
GSEA	PMID:17644558	http://www.gsea-msigdb.org/gsea/msigdb/index.jsp
enrichR database	Maayanlab	https://maayanlab.cloud/Enrichr/
Dextramers		
HLA-A*0201 (NLVPMVATV), APC CMV Dextramer	Immudex	WB2132- APC-150
HLA-A*0201 (GLCTLVAML), APC EBV Dextramer	Immudex	WB2130- APC-150
HLA-A*0201 LLYNCCYHV (HAV) dCODE Dextramer® grade (Gold)	Immudex	dCODELLYNCCYHV - 50T
HLA-A*0201 NLVPMVATV (CMV) dCODE	Immudex	dCODENLVPMVATV -

Dextramer® grade (Gold)		50T
HLA-A*0201 GLCTLVAML (EBV) dCODE Dextramer® grade (Gold)	Immudex	dCODEGLCTLVAML - 50T
HLA-A*0201 GILGFVFTL (IAV) dCODE Dextramer® grade (Gold)	Immudex	dCODEGILGFVFTL50 T

434

435 **STUDY PARTICIPANT DETAILS**

436 **Human blood samples**

437 Peripheral blood samples were obtained from healthy volunteers from KAIST Clinic
438 Pappalardo Center, who were not taking any immunosuppressive medications. Peripheral
439 blood samples were also collected from patients with acute HAV infection and also during
440 the convalescent phase, who at admission exhibited clinical and laboratory features of acute
441 hepatitis A (AHA), including seropositivity for anti-HAV IgM and/or IgG antibodies. PBMCs
442 were isolated from whole blood by density gradient centrifugation using Lymphocytes
443 Separation Medium (Corning). The isolated PBMCs were cryopreserved in freezing media
444 containing fetal bovine serum (Corning) with 10% dimethyl sulfoxide (Sigma-Aldrich) until
445 their use. This study was conducted in accordance with the principles of the Declaration of
446 Helsinki, and was approved by the institutional review board of each involved institution
447 (KAIST: KH2018-118 and Chungnam National University Hospital: 2019-03-066-025). Each
448 healthy volunteer and patient with HAV infection gave their written informed consent prior
449 to inclusion in the study.

450

451 **METHOD DETAILS**

452 **Cell sorting**

453 $CD8^+$ T cells were negatively isolated from PBMCs of healthy donors and patients with HAV
454 infection using a $CD8^+$ T-cell isolation kit (Miltenyi Biotec), according to the manufacturer's
455 instructions. Isolated $CD8^+$ T cells were stained with FITC-conjugated anti-CCR7 antibody
456 (R&D systems), and then further stained with anti-FITC microbeads (Miltenyi Biotec),
457 following the manufacturer's instructions for negatively isolating $CCR7^-$ memory $CD8^+$ T
458 cells.

459

460 **In vitro stimulation and proliferation assay**

461 PBMCs were cultured in RPMI 1640 medium (Corning) supplemented with 10% fetal bovine
462 serum (Corning) and 1% penicillin/streptomycin (Sigma-Aldrich). PBMCs were cultured for 48
463 hours with IL-2 (10 ng/ml; Peprotech), IL-4 (10 ng/ml; R&D systems), IL-7 (10 ng/ml;
464 Peprotech), IL-9 (10 ng/ml; Peprotech), IL-15 (10 ng/ml; Peprotech), or IL-21 (10 ng/ml;
465 Peprotech), and we examined the NKG2D expression among $CD8^+$ T cells and their naïve and
466 memory subsets. Sorted $CCR7^-$ memory $CD8^+$ T cells were cultured with IL-15 (10 ng/ml),
467 anti-CD3 (coated, 1 µg/ml; Invitrogen), PMA (10 ng/ml; Sigma-Aldrich), ionomycin (500
468 ng/ml; Sigma-Aldrich), or combinations of these additives, for 48 hours followed by analysis
469 of NKG2D and granzyme B expressions, or for 96 hours followed by analysis of CD38 and
470 HLA-DR expressions.

471 For a proliferation assay, sorted $CCR7^-$ memory $CD8^+$ T cells were stained with
472 CellTrace Violet (Invitrogen) following the manufacturer's instructions. CellTrace Violet-
473 labelled cells were cultured with IL-15 (10 ng/ml), anti-CD3 (coated, 1 µg/ml), or the
474 combination of both for 96 hours, and then we measured their proliferation and Ki-67
475 expression.

476 We also tested the effects of chemical inhibitors. Sorted $CCR7^-$ memory $CD8^+$ T cells
477 were pre-treated with everolimus (10 µM; Selleckchem), FK506 (10 ng/ml; Selleckchem), CsA
478 (100 ng/ml; Selleckchem), SP600125 (10 µM; Selleckchem), or SR11302 (10 µM;
479 Selleckchem) for one hour, followed by stimulation with IL-15, anti-CD3, or the combination
480 of both.

481

482 **Flow cytometry**

483 Cells were stained with a mixture of brilliant stain buffer (BD Biosciences) and fluorochrome-
484 conjugated antibodies that bind to surface markers, for 20 min at 4°C. Dead cells were
485 excluded from analysis using the Live/Dead Cell Stain Kit (Invitrogen). To stain intracellular
486 molecules, surface-stained cells were fixed and permeabilized (Invitrogen) for 20 min at 4°C.
487 Subsequently, these cells were stained with fluorochrome-conjugated antibodies targeting
488 intracellular molecules, for 20 min at 4°C. To analyze HCMV- and EBV-specific $CD8^+$ T cells,
489 PBMCs were stained with MHC-I dextramers (Immudex) specific for HCMV (HCMV pp65
490 495–504; NLVPMVATV) and EBV (EBV BMLF-1 259–267; GLCTLVAML), and fluorochrome-

491 conjugated monoclonal antibodies for cell surface proteins. Multicolor flow cytometry was
492 performed using LSR II, LSR Fortessa, and FACSymphony A3 instruments (BD Biosciences),
493 and data were analyzed using FlowJo software (Treestar).
494
495 **Bulk RNA sequencing**
496 Bulk RNA-seq was performed on sorted CCR7^{-} memory CD8^{+} T cells that were stimulated
497 with IL-15, anti-CD3, or a combination of both for 48 hours; or with IL-15, ionomycin, or a
498 combination of both for 12 hours. Total RNA was extracted using TRIZOL reagent
499 (Invitrogen). RNA quality and quantity were evaluated using an Agilent 2100 Bioanalyzer
500 with an RNA 6000 Nano Chip (Agilent Technologies) and an ND-2000 spectrophotometer
501 (Thermo Fisher Scientific), respectively. An RNA library was prepared using a QuantSeq 3'
502 mRNA-seq Library Prep Kit (Lexogen). An individual set of 500 ng total RNA was prepared, an
503 oligo-dT primer containing an Illumina-compatible sequence at its 5' end was hybridized to
504 the RNA, and reverse transcription was performed. After degradation of the RNA template,
505 second strand synthesis was processed using a random primer with an Illumina-compatible
506 linker sequence at its 5' end. Magnetic beads were used to purify the double-stranded
507 library, and to eliminate reactive components. The library was amplified for the addition of
508 complete adapter sequences needed for cluster generation and, finally, the amplified library
509 was purified from PCR components.
510 High-throughput sequencing was performed by single-end 75 sequencing using
511 NextSeq 500 (Illumina). Alignment of the QuantSeq 3' mRNA-Seq reads based on a human
512 reference sequence (hg19) was performed using Bowtie2[45]. Gene counts were normalized
513 according to the library size, and DEGs were analyzed using DESeq2 (v.1.24.0)[46]. An
514 experimental batch was corrected using the removeBatchEffect function from limma[47]. DEGs
515 were identified based on two cut-off values: an adjusted *P* value < 0.05, and an absolute log2
516 fold change > 1. GSEA was performed using Broad Institute Software (http://www.gsea-
517 msigdb.org/gsea/index.jsp). For upregulated DEGs, pathway analysis was performed using
518 the enrichR database (https://maayanlab.cloud/Enrichr/). The following pathway databases
519 were utilized in this study: MSigDB Hallmark 2020 (interferon gamma response, interferon
520 alpha response, and TNF-alpha signaling via NF-kB), Reactome 2022 (interferon signaling R-
521 HAS-913531, cell cycle R-HAS-1640170, rRNA processing, cytokine signaling in immune

522 system R-HAS-1280215, innate immune system R-HAS-168249, and interferon alpha/beta
523 signaling R-HAS-909733), KEGG 2021 Human (natural killer cell-mediated cytotoxicity, T-cell
524 receptor signaling pathway, and chemokine signaling pathway), Elsevier Pathway Collection
525 (natural killer cell precursor -> NK cell surface expression markers, natural killer cell
526 activation), NCI-Nature 2016 (calcineurin-regulated NFAT-dependent transcription in
527 lymphocyte), and BioPlanet 2019 (regulation of NFAT transcription factors, MYC active
528 pathway, EGFR1 pathway, T-cell receptor calcium pathway).
529
530 **Cytotoxicity assay**
531 Sorted $CD8^+$ T cells from patients with acute HAV infection were stimulated with IL-15 (10
532 ng/ml) alone or in combination with ionomycin (500 ng/ml) for 24 hours. K562 target cells
533 were labelled with PKH26 (Sigma-Aldrich) following the manufacturer's instructions, and co-
534 cultured with stimulated $CD8^+$ T cells at an effector:target cell ratio of 20:1, for 12 hours. To-
535 Pro-3-iodide (0.5 µM; Invitrogen) was added to the samples, and cells were immediately
536 analyzed by flow cytometry. To obtain the background or maximum To-Pro-3-Iodide staining,
537 target cells were incubated in medium without effector cells or detergent, respectively. The
538 specific cytotoxicity was calculated by extracting the percentage of To-Pro-3-Iodide+ PKJ26+
539 cells cultured without effector cells, from the percentage of To-Pro-3-Iodide+ $PKH26^+$ cells in
540 co-culture.
541
542 **siRNA transfection**
543 PBMCs were transfected with c-Jun- or c-Fos-specific small interfering RNA (siRNA)
544 (Invitrogen) or negative control siRNA (Invitrogen) using the Neon NxT electroporation
545 system (Invitrogen). Transfection was performed with 200 nM siRNA at 2000 V for three 10
546 ms pulses. Following transfection, PBMCs were cultured in RPMI 1640 medium (Corning)
547 supplemented with 10% fetal bovine serum (Corning) without antibiotics for 4 days.
548 Subsequently, PBMCs were treated with IL-15 (10 ng/ml) for 48 hours, and expression of
549 NKG2D was analyzed on $CCR7^-$ memory $CD8^+$ T cells by flow cytometry.
550
551 **NFATc1 plasmids transfection**
552

553 pcDNA3.1 plasmid containing wild-type and T551A mutant[23] NFATc1 were purchased from
554 Genescript. PBMCs were transfected with empty pcDNA3.1 plasmids or plasmids containing
555 wild-type and T551A mutant NFATc1 using the Neon NxT electroporation system.
556 Transfection was performed with 5 µg of plasmids at 2000 V for a single 20 ms pulse.
557 Subsequently, PBMCs were cultured with IL-15 (10 ng/ml) for 48 hours and expression of
558 NKG2D was analyzed on $CCR7^{-}$ memory $CD8^{+}$ T cells by flow cytometry.
559
560 **scRNA-seq library preparation and sequencing**
561 Sorted $CD8^{+}$ T cells from PBMCs of patients (*n* = 5) at acute and convalescent stages of HAV
562 infection and healthy donors (*n* = 3) were stained with PE-conjugated MHC-I dCODE
563 dextramers (Immudex) specific for HLA-A*0201 HAV $3D_{2026}$ LLYNCCYHV, HLA-A*0201 HCMV
564 $pp65_{495}$ NLVPMVATV, HLA-A*0201 EBV $BMLF1_{259}$ GLCTLVAML, and HLA-A*0201 IAV MP_{58}
565 GILGFVFTL. Subsequently, these cells were sorted into dCODE-positive and -negative $CD8^{+}$ T
566 cells using a FACSAria II instrument (BD Biosciences). The sorted cells were mixed at a 1:9
567 ratio, and then further stained with CITE-seq antibodies (TotalSeq-C; Biolegend). Cell
568 suspensions were pelleted, and scRNA-seq libraries were prepared using the Chromium
569 Single Cell 5' Library & Gel Bead Kit (PN-10000006) and 5' Feature Barcode Library Kit (PN-
570 1000020) (10X Genomics), following the manufacturer's instructions. These libraries were
571 sequenced at a depth of approximately 20,000 reads per cell for genes and antibody-derived
572 tags (ADTs) using the NovaSeq6000 platform (Illumina).
573
574 **Single-cell transcriptome and ADT expression analysis**
575 Fastq files were generated by demultiplexing the sequenced data using the mkfastq function
576 (Cell Ranger, 10X Genomics, v3.1.0). The demultiplexed fastq files for the expressions of each
577 gene and ADT were aligned to the reference human genome (GRCH38; 10X Cell Ranger
578 reference GRCh38 v3.0.0). The barcode sequencing of each ADT and dCODE dextramer,
579 filtering, barcode counting, and UMI counting were performed to generate feature-barcode
580 matrices using the count function (Cell Ranger, v3.1.0). For basic quality control, we filtered
581 out low-quality cells with mitochondrial genes constituting >10% of their total gene
582 expression, <300 genes or >5,500 genes, or UMI counts of <500 or >55,000. Next, we
583 identified highly variable genes by standardizing the normalization of gene expression in

each cell based on the total read count. To correct for a batch effect and harmonize the datasets, we identified 'anchor' vectors of genes using the FindIntegrationAnchors function, and integrated the datasets using the IntegrateData function (Seurat, v3.2.2)[48]. The integrated samples were scaled using the ScaleData function (Seurat), and PCA was conducted using the RunPCA function (Seurat) for dimensional reduction. Lastly, the cells were visualized by UMAP using the top 20 principal components (PCs) with the RunUMAP function (Seurat) for whole-cell types. Enrichment of bulk RNA-seq data on scRNA-seq data was performed by measuring the enrichment score with the Addmodulescore function (Seurat). The pseudo-bulk scRNA-seq data were obtained using the AggregateExpression function (Seurat).

Analysis of a public RNA-seq dataset

We re-analyzed publicly available bulk RNA-seq datasets for bystander-activated $CD8^+$ T cells from a mouse model of influenza infection[20] (SRX13530605, SRX13530604, SRX13530603, SRX13530601, and SRX13530600ref). Orthologous pairs of human and mouse genes were processed using the getLDS function (biomaRt)[49]. Enrichment of upregulated DEGs from the current study in the public data was performed using the fgsea package

Statistical analysis

Statistical analyses were performed using GraphPad Prism (GraphPad Software version 8.4) or R software (R Foundation for Statistical Computing). The paired t test was used to compare continuous variables. The Mann–Whitney U test was used to compare data between two unpaired groups, and the Wilcoxon signed-rank test was used to compare data between two paired groups. Two-sided *P* values were determined in all analyses, and a *P* value < 0.05 was considered significant.

Figure 1

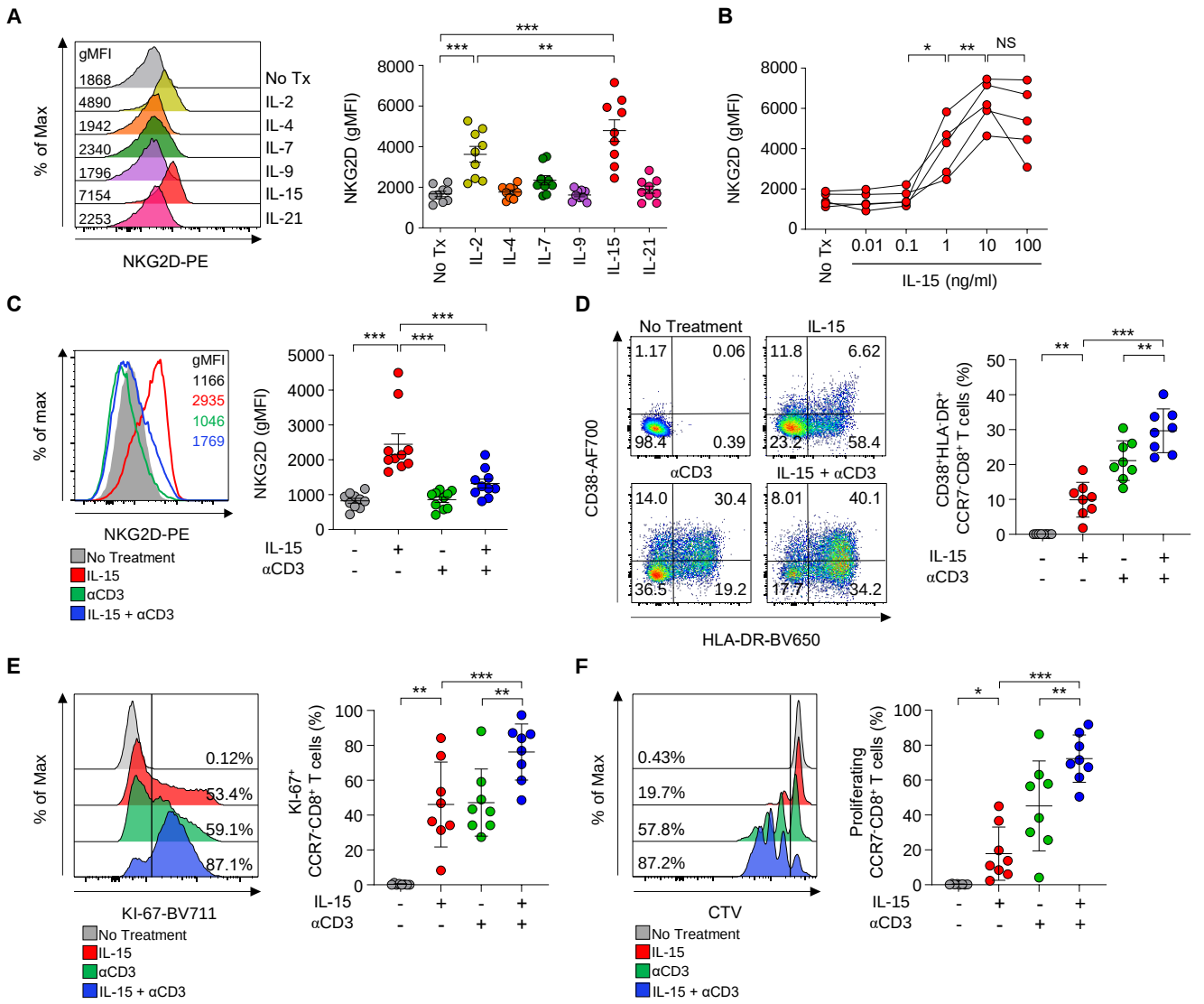

Figure 1. IL-15-induced upregulation of NKG2D on memory CD8⁺ T cells, which is counteracted by concurrent TCR stimulation. (**A** and **B**) Peripheral blood mononuclear cells (PBMCs) from healthy donors (n = 9) were stimulated for 48 hours with IL-2 (10 ng/ml), IL-4 (10 ng/ml), IL-7 (10 ng/ml), IL-9 (10 ng/ml), IL-15 (10 ng/ml) or IL-21 (50 ng/ml). (A) Representative figures and cumulative data presenting NKG2D expression on CCR7⁻ memory CD8⁺ T cells from healthy donor PBMCs following stimulation with indicated cytokines. (B) NKG2D expression on CCR7⁻ memory CD8⁺ T cells stimulated for 48 hours with varying doses of IL-15 (0.01, 0.1, 1, 10, and 100 ng/ml). (**C** and **D**) Sorted CCR7⁻ memory CD8⁺ T cells from healthy donors were stimulated with IL-15 (10 ng/ml), anti-CD3 (coated, 1 µg/ml), or the combination of both. Representative figures and cumulative data presenting the expression of (C) NKG2D (n = 10) and (D) CD38 and HLA-DR (n = 8) on CCR7⁻ memory CD8⁺ T cells upon stimulation for 48 hours and 96 hours, respectively. (**E** and **F**) Sorted CCR7⁻ memory CD8⁺ T cells from healthy donors (n = 8) were stained with CellTrace Violet, and stimulated with IL-15 (10 ng/ml), anti-CD3 (coated, 1 µg/ml), or the combination of both. After 96 hours of stimulation, we measured the (E) Ki-67 expression and (F) proliferation of CCR7⁻ memory CD8⁺ T cells. Error bars represent mean ± SD. Statistical analysis was performed using the paired Student's t test. NS, not significant, *P < 0.05, **P < 0.01, ***P < 0.001.

Figure 2

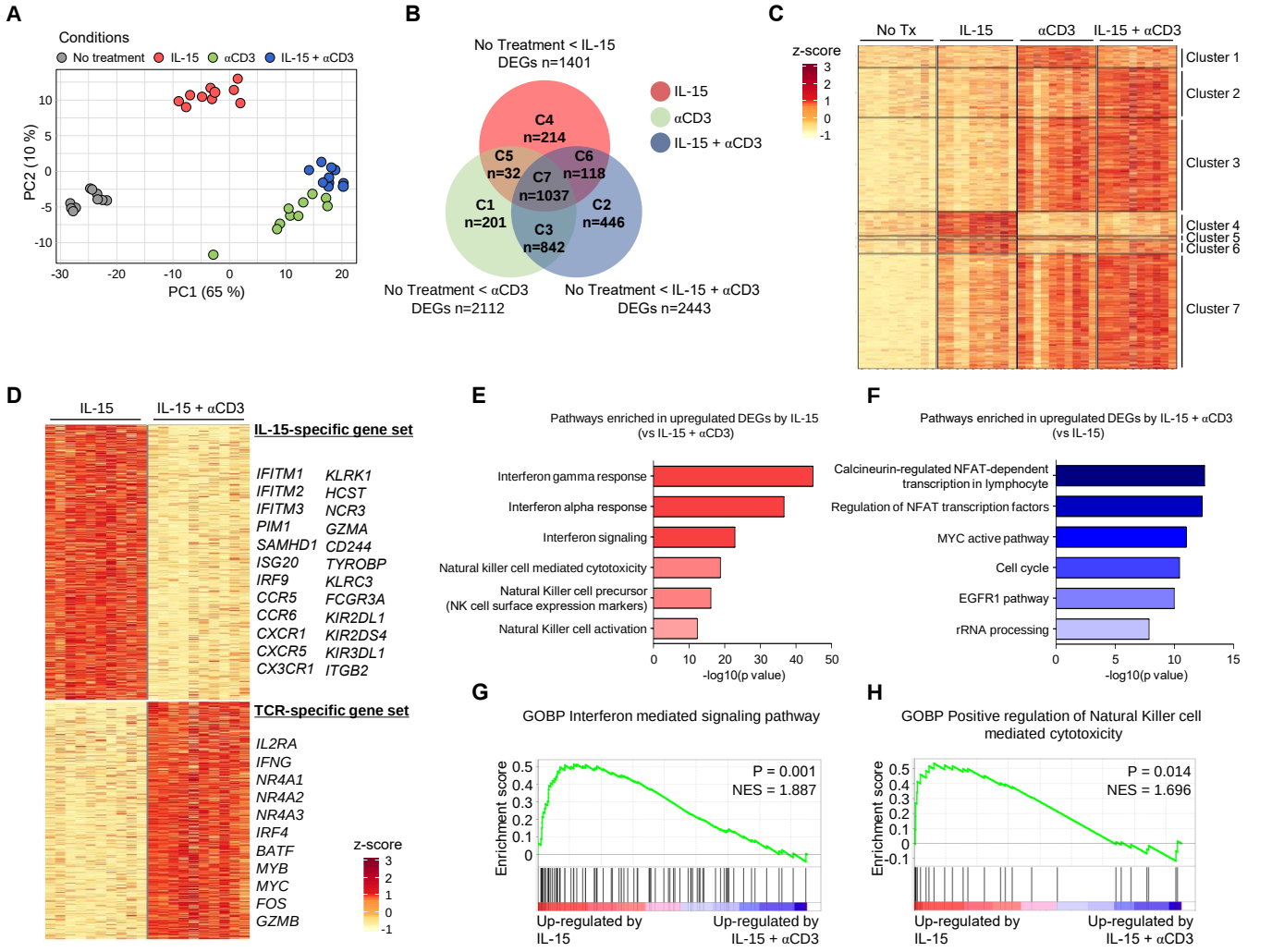

Figure 2. Transcriptional profiles of memory CD8⁺ T cells stimulated with IL-15, anti-CD3, or the combination of both. (**A-H**) Sorted CCR7⁻ memory CD8⁺ T cells from healthy donors (n = 10) were stimulated for 48 hours with IL-15 (10 ng/ml), anti-CD3 (coated, 1 µg/ml), or the combination of both. Total RNA was isolated and RNA-seq was performed. (**A**) Principal component analysis (PCA) indicating segregation of the gene expression patterns of memory CD8⁺ T cells stimulated with IL-15, anti-CD3, or the combination of both. (**B**) Venn diagram of individual and overlapping differentially expressed genes of memory CD8⁺ T cells stimulated with IL-15, anti-CD3, or the combination of both, compared to unstimulated cells and (**C**) Heat-map showing the z scores of normalized read counts (adjusted $P < 0.05$, Log2 fold-change > 1). (**D**) Heat-map of differentially expressed genes between memory CD8⁺ T cells stimulated with IL-15 alone or IL-15 plus anti-CD3 (adjusted $P < 0.05$, Log2 fold-change > 1). (**E** and **F**) Bar-plots showing the enrichment scores (−log10[p value]) of various pathways enriched in DEGs upregulated by (E) IL-15 or (F) IL-15 plus anti-CD3. (**G** and **H**) GSEA of (G) GOBP interferon-mediated signaling pathway (GO: 0140888) and (H) GOBP positive regulation of natural killer-cell-mediated cytotoxicity (GO: 0045954) in memory CD8⁺ T cells stimulated with IL-15 alone versus IL-15 plus anti-CD3.

Figure 3

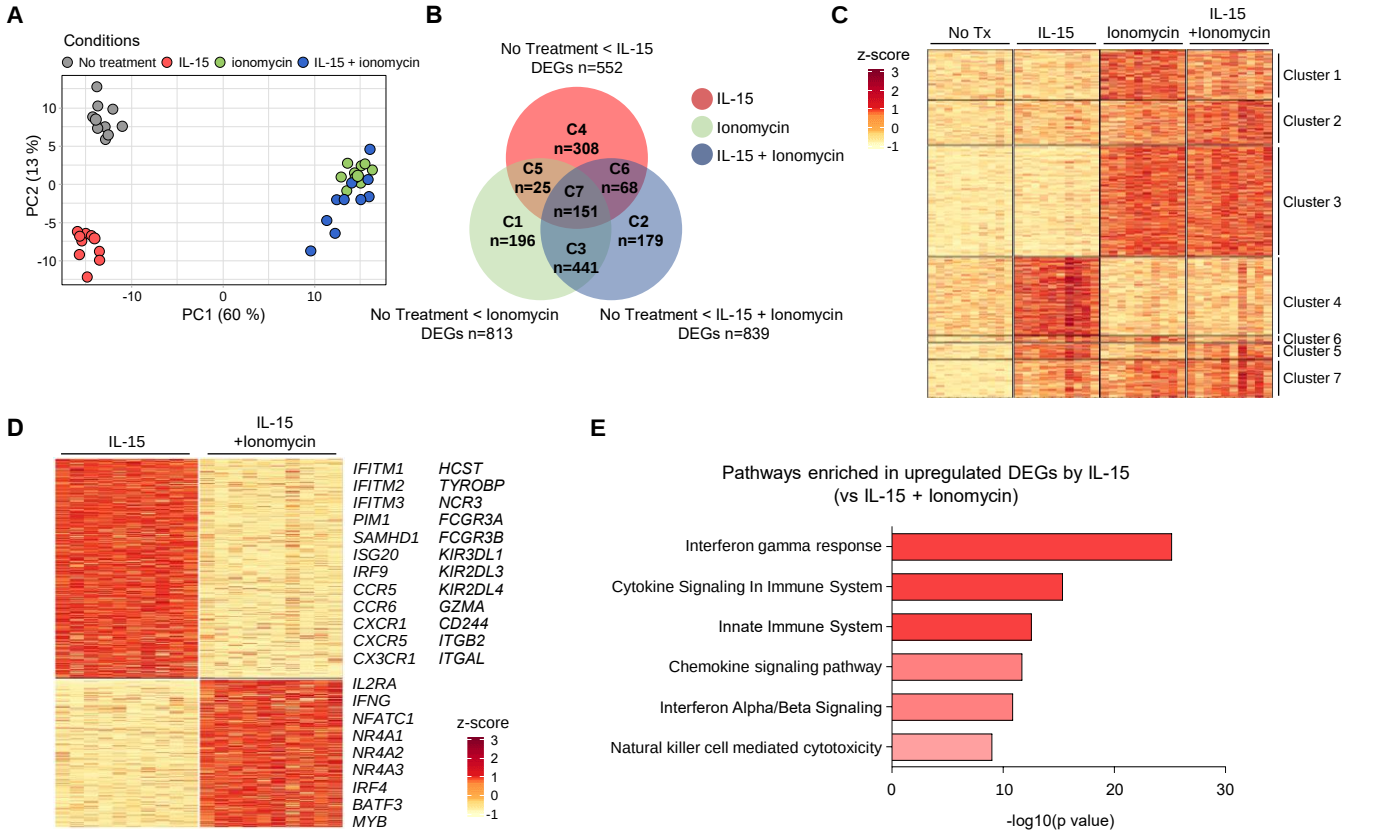

Figure 3. Transcriptional profiles of memory CD8⁺ T cells stimulated with IL-15, ionomycin, or the combination of both. (**A-E**) Sorted CCR7⁻ memory CD8⁺ T cells from healthy donors (n = 10) were stimulated for 12 hours with IL-15 (10 ng/ml), ionomycin (500 ng/ml), or the combination of both. Total RNA was isolated and RNA-seq was performed. (**A**) PCA indicating segregation of gene expression patterns of memory CD8⁺ T cells stimulated with IL-15, ionomycin, or the combination of both. (**B**) Venn diagram of individual and overlapping differentially expressed genes of memory CD8⁺ T cells stimulated with IL-15, ionomycin, or the combination of both compared to unstimulated cells and (**C**) Heat-map showing the z scores of normalized read counts (adjusted $P < 0.05$, Log2 fold-change > 1). (**D**) Heat-map of differentially expressed genes between memory CD8⁺ T cells stimulated with IL-15 or with IL-15 plus ionomycin (adjusted $P < 0.05$, Log2 fold-change > 1). (**E**) Bar-plots showing the enrichment scores (−log10[p value]) of various pathways enriched in DEGs upregulated by IL-15 and down-regulated by IL-15 plus ionomycin. Statistical analysis was performed using the paired Student's t test. ****$P < 0.0001$.

Figure 4

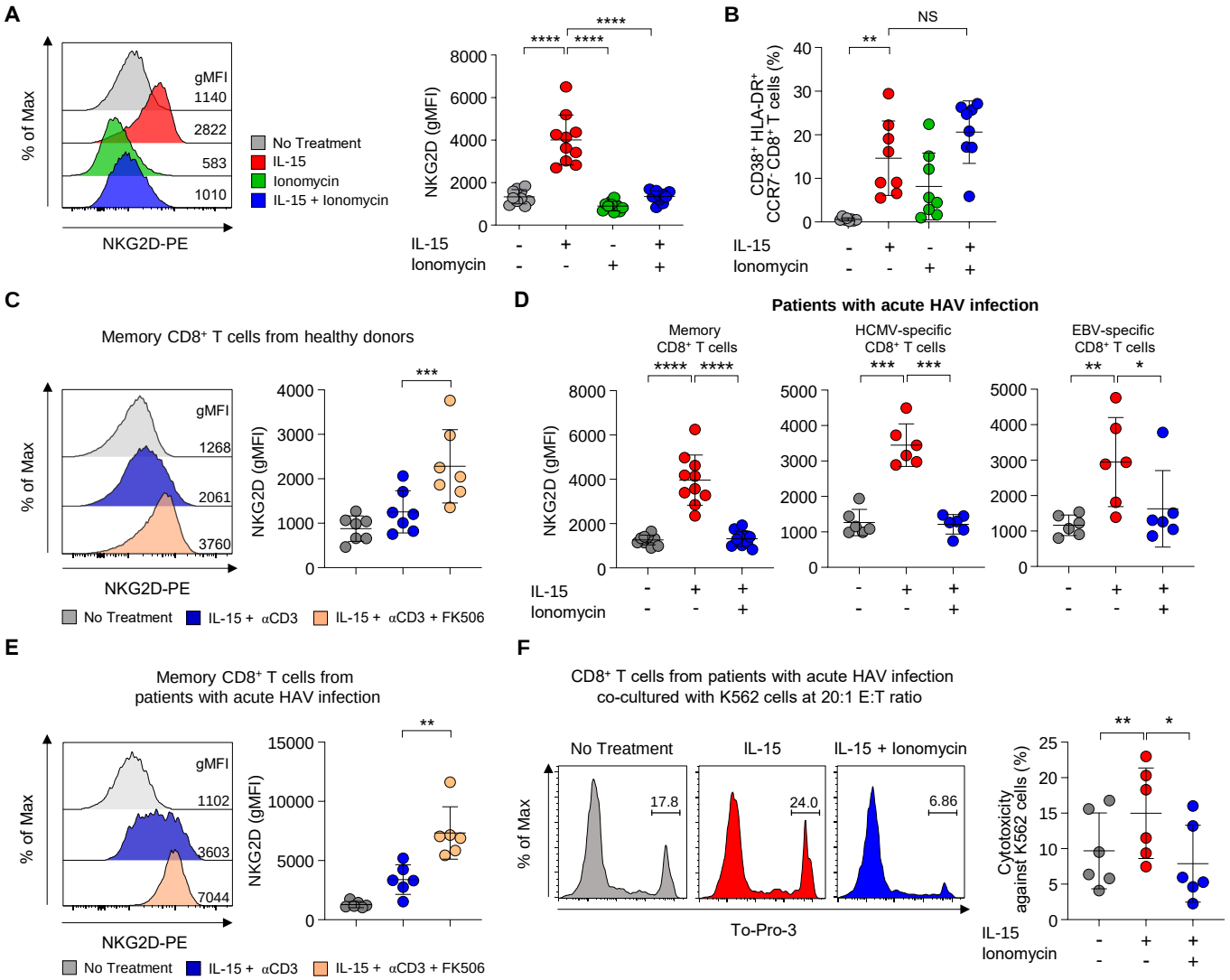

Figure 4. The role of Ca^{2+}-calcineurin signaling on IL-15-induced innate-like cytotoxicity of $CD8^+$ T cells. (**A** and **B**) Sorted $CCR7^-$ memory $CD8^+$ T cells from healthy donors were stimulated with IL-15 (10 ng/ml), ionomycin (500 ng/ml), or the combination of both. Representative figures and cumulative data presenting the expression of (A) NKG2D (n = 10) and (B) CD38 and HLA-DR (n = 8) on $CCR7^-$ memory $CD8^+$ T cells after 48 hours and 96 hours of stimulation, respectively. (**C**) Sorted $CCR7^-$ memory $CD8^+$ T cells from healthy donors (n = 7) were pretreated with FK506 (10 ng/ml) for 1 hour, and then stimulated with IL-15 (10 ng/ml) and anti-CD3 (coated, 1 µg/ml). After 48 hours of stimulation, NKG2D expression was measured on $CCR7^-$ memory $CD8^+$ T cells. (**D**) PBMCs from patients with acute HAV infection were stimulated for 24 hours with IL-15 (10 ng/ml) or a combination of IL-15 plus ionomycin (500 ng/ml). After 48 hours of stimulation, NKG2D expression was measured on $CCR7^-$ memory (n = 10) , HCMV-specific (n = 6), and EBV-specific (n = 6) $CD8^+$ T cells. (**E**) Sorted $CCR7^-$ memory $CD8^+$ T cells from patients with acute HAV infection (n = 6) were cultured as in (C) and NKG2D expression was measured on $CCR7^-$ memory $CD8^+$ T cells. (**F**) Sorted total $CD8^+$ T cells from patients with acute HAV infection (n = 6) were stimulated with IL-15 (10 ng/ml) or a combination of IL-15 plus ionomycin (500 ng/ml) for 24 hours, and co-cultured with PKH-26-labeled K562 cells at a 20:1 effector:target cell (E:T) ratio for 12 hours. Cytotoxicity was analyzed by flow cytometry following staining of the dead cells with TO-PRO-3. Error bars represent mean ± SD. Statistical analysis was performed using the paired Student's t test. *P < 0.05, **P < 0.01, ***P < 0.001, ****P < 0.0001.

Figure 5

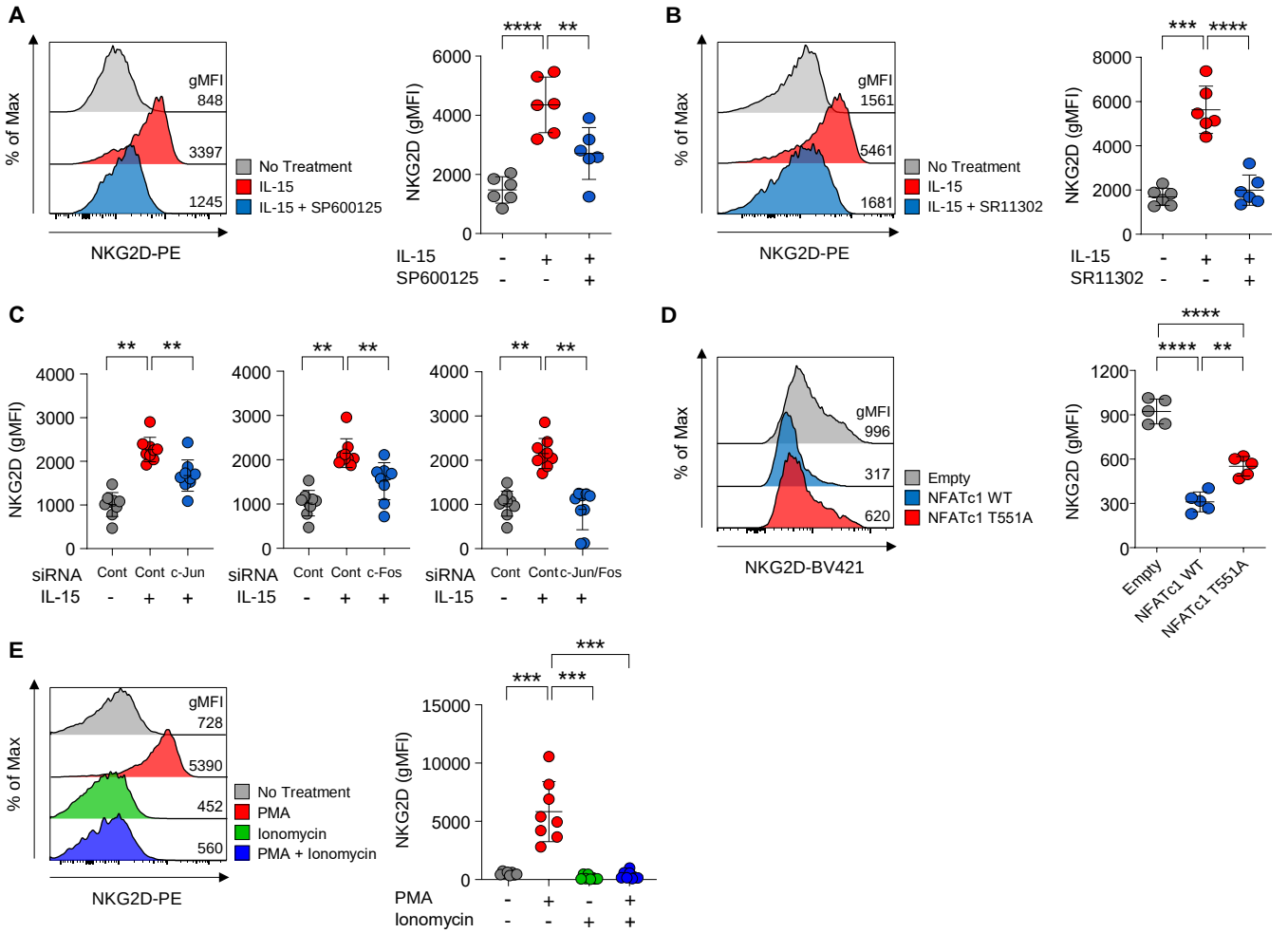

Figure 5. NFATc1-mediated suppression of IL-15-induced NKG2D upregulation through AP-1 binding. PBMCs from healthy donors (*n* = 6) were pretreated with (**A**) SP600125 (10 µM) or (**B**) SR11302 (10 µM) for 1 hour, and then stimulated with IL-15 (10 ng/ml). After 48 hours of stimulation, NKG2D expression was measured on CCR7⁻ memory CD8⁺ T cells. (**C**) PBMCs from healthy donors (*n* = 9) were transfected with c-Jun siRNA (200 nM), c-Fos siRNA (200 nM) or the combination of both siRNAs and rested for 4 days. Subsequently, PBMCs were stimulated with IL-15 (10 ng/ml) for 48 hours and NKG2D expression was measured on CCR7⁻ memory CD8⁺ T cells. (**D**) PBMCs from healthy donors (*n* = 5) were transfected with pcDNA3.1 plasmids containing wild-type or T551A mutant NFATc1. Subsequently, PBMCs were stimulated with IL-15 (10 ng/ml) for 48 hours and NKG2D expression was measured on CCR7⁻ memory CD8⁺ T cells. (**E**) Sorted CCR7⁻ memory CD8⁺ T cells from healthy donors (*n* = 8) were stimulated with PMA (10 ng/ml), ionomycin (500 ng/ml), or the combination of both for 48 hours and NKG2D expression was measured. Error bars represent mean ± SD. Statistical analysis was performed using the paired Student's t test. ***P* < 0.01, ****P* < 0.001, *****P* < 0.0001.

Figure 6

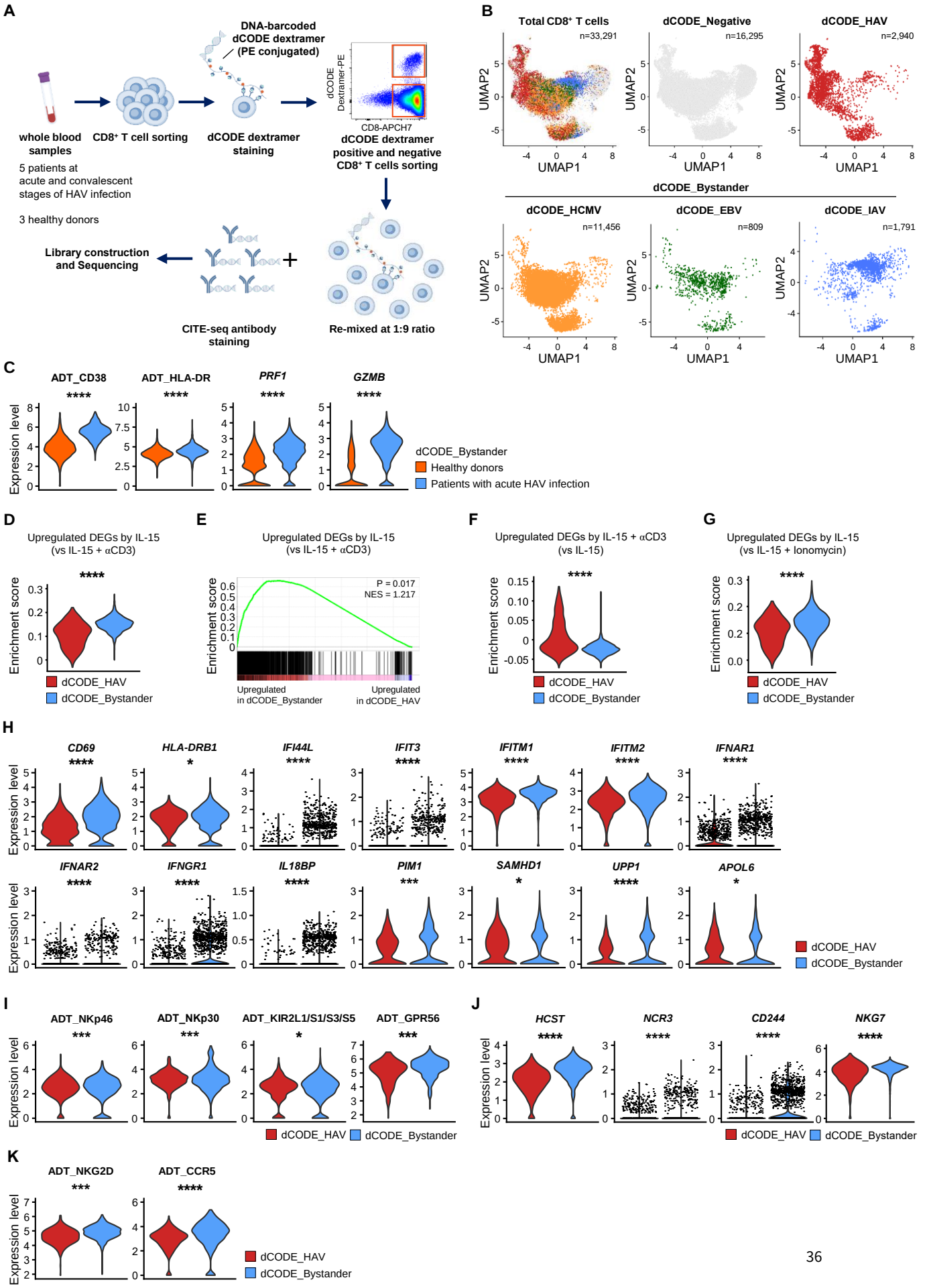
A
DNA-barcoded dCODE dextramer (PE conjugated)
whole blood samples
CD8+ T cell sorting
dCODE dextramer staining
dCODE Dextramer-PE
CD8-APCH7
dCODE dextramer positive and negative CD8+ T cells sorting
5 patients at acute and convalescent stages of HAV infection
3 healthy donors
Library construction and Sequencing
CITE-seq antibody staining
Re-mixed at 1:9 ratio
B
Total CD8+ T cells
n=33,291
dCODE_Negative
n=16,295
dCODE_HAV
n=2,940
dCODE_Bystander
dCODE_HCMV
n=11,456
dCODE_EBV
n=809
dCODE_IAV
n=1,791
UMAP1
UMAP2
C
ADT_CD38
ADT_HLA-DR
PRF1
GZMB
Expression level
dCODE_Bystander
Healthy donors
Patients with acute HAV infection
D
Upregulated DEGs by IL-15 (vs IL-15 + αCD3)
Enrichment score
dCODE_HAV
dCODE_Bystander
E
Upregulated DEGs by IL-15 (vs IL-15 + αCD3)
P = 0.017
NES = 1.217
Upregulated in dCODE_Bystander
Upregulated in dCODE_HAV
F
Upregulated DEGs by IL-15 + αCD3 (vs IL-15)
G
Upregulated DEGs by IL-15 (vs IL-15 + Ionomycin)
H
CD69
HLA-DRB1
IFI44L
IFIT3
IFITM1
IFITM2
IFNAR1
IFNAR2
IFNGR1
IL18BP
PIM1
SAMHD1
UPP1
APOL6
I
ADT_NKp46
ADT_NKp30
ADT_KIR2L1/S1/S3/S5
ADT_GPR56
J
HCST
NCR3
CD244
NKG7
K
ADT_NKG2D
ADT_CCR5

Figure 6 (continued)

Figure 6. High-throughput single-cell analysis of virus-specific CD8$^+$ T cells from patients with HAV infection. (**A-K**) Total CD8$^+$ T cells were isolated from patients at acute and convalescent stages of HAV infection (*n* = 5) and healthy donors (*n* = 3) by magnetic separation, and stained with DNA barcode-labeled MHC class I dextramers conjugated with PE (dCODE dextramers). dCODE dextramer-positive and -negative CD8$^+$ T cells were flow-sorted, and then re-mixed at a 1:9 ratio and further stained with CITE-seq/antibody-derived tag (ADT) antibodies. Subsequently, these cells were processed for single-cell RNA sequencing. (**A**) Schematic overview of the experimental design. (**B**) UMAP projections of 33,291 dCODE-negative (*n* = 16,295) and HAV-specific CD8$^+$ T cells (*n* = 2,940), and bystander CD8$^+$ T cells, including HCMV-specific (*n* = 11,456), EBV-specific (*n* = 809) and IAV-specific (*n* = 1,791) CD8$^+$ T cells. (**C**) Violin plots showing ADT expression of CD38 and HLA-DR, and normalized gene expression of PRF1 and GZMB between bystander CD8$^+$ T cells from acute HAV infection patients versus healthy donors. (**D**) Violin plot showing enrichment score for DEGs upregulated by stimulation with IL-15 compared to with IL-15 plus anti-CD3 in memory CD8$^+$ T cells, compared between HAV-specific and bystander CD8$^+$ T cells from patients with acute HAV infection. (**E**) GSEA of upregulated DEGs from IL-15-stimulated memory CD8$^+$ T cells, using the transcriptomes of HAV-specific versus bystander CD8$^+$ T cells from patients with acute HAV infection obtained using a pseudo bulk approach. (**F**) Violin plot showing enrichment score for DEGs upregulated by stimulation with IL-15 and IL-15 plus anti-CD3 in memory CD8$^+$ T cells, compared between HAV-specific and bystander CD8$^+$ T cells from patients with acute HAV infection. (**G**) Violin plot showing enrichment score for DEGs upregulated by stimulation with IL-15 compared to IL-15 plus ionomycin in memory CD8$^+$ T cells, compared between HAV-specific and bystander CD8$^+$ T cells from scRNA-seq analysis of patients with acute HAV infection. (**H**) Violin plots showing normalized expression of genes that are associated with IFN response in HAV-specific versus bystander CD8$^+$ T cells from patients with acute HAV infection. (**I and J**) Violin plots showing (I) ADT expression of NKp46, NKp30, KIR2L1/S1/S3/S5, and GPR56 and (J) normalized gene expression of HCST, NCR3, CD244, and NKG7 in HAV-specific versus bystander CD8$^+$ T cells from patients with acute HAV infection. (**K**) ADT expression of NKG2D and CCR5 in HAV-specific versus bystander CD8$^+$ T cells from patients with acute HAV infection. Statistical analysis was performed using the Mann-Whitney U-test *P < 0.05, ***P < 0.001, ****P < 0.0001.

References

1. Kaech, S.M., Wherry, E.J. & Ahmed, R. Effector and memory T-cell differentiation: implications for vaccine development. *Nat Rev Immunol*. **2**, 251-262 (2002).
2. Lee, H., Jeong, S. & Shin, E.C. Significance of bystander T cell activation in microbial infection. *Nat Immunol*. **23**, 13-22 (2022).
3. Maurice, N.J., Taber, A.K. & Prlic, M. The Ugly Duckling Turned to Swan: A Change in Perception of Bystander-Activated Memory CD8 T Cells. *J Immunol*. **206**, 455-462 (2021).
4. Zhang, X.H., Sun, S.Q., Hwang, I.K., Tough, D.F. & Sprent, J. Potent and selective stimulation of memory-phenotype CD8(+) T cells in vivo by IL-15. *Immunity*. **8**, 591-599 (1998).
5. Meresse, B. et al. Coordinated induction by IL15 of a TCR-independent NKG2D signaling pathway converts CTL into lymphokine-activated killer cells in celiac disease. *Immunity*. **21**, 357-366 (2004).
6. Soudja, S.M., Ruiz, A.L., Marie, J.C. & Lauvau, G. Inflammatory monocytes activate memory CD8(+) T and innate NK lymphocytes independent of cognate antigen during microbial pathogen invasion. *Immunity*. **37**, 549-562 (2012).
7. Younes, S.A. et al. IL-15 promotes activation and expansion of CD8+ T cells in HIV-1 infection. *J Clin Invest*. **126**, 2745-2756 (2016).
8. Kim, J. et al. Innate-like Cytotoxic Function of Bystander-Activated CD8(+) T Cells Is Associated with Liver Injury in Acute Hepatitis A. *Immunity*. **48**, 161-173 e165 (2018).
9. Sandalova, E. et al. Contribution of herpesvirus specific CD8 T cells to anti-viral T cell response in humans. *PLoS Pathog*. **6**, e1001051 (2010).
10. Leem, G. et al. Tumour-infiltrating bystander CD8(+) T cells activated by IL-15 contribute to tumour control in non-small cell lung cancer. *Thorax*. **77**, 769-780 (2022).
11. Chu, T. et al. Bystander-activated memory CD8 T cells control early pathogen load in an innate-like, NKG2D-dependent manner. *Cell Rep*. **3**, 701-708 (2013).
12. Ge, C. et al. Bystander Activation of Pulmonary Trm Cells Attenuates the Severity of Bacterial Pneumonia by Enhancing Neutrophil Recruitment. *Cell Rep*. **29**, 4236-4244 e4233 (2019).
13. Sckisel, G.D. et al. Influenza infection results in local expansion of memory CD8(+) T cells with antigen non-specific phenotype and function. *Clin Exp Immunol*. **175**, 79-91 (2014).

14. Arkatkar, T. et al. Memory T cells possess an innate-like function in local protection from mucosal infection. *J Clin Invest*. **133** (2023).
15. Ostler, T., Pircher, H. & Ehl, S. "Bystander" recruitment of systemic memory T cells delays the immune response to respiratory virus infection. *Eur J Immunol*. **33**, 1839-1848 (2003).
16. Crosby, E.J., Goldschmidt, M.H., Wherry, E.J. & Scott, P. Engagement of NKG2D on bystander memory CD8 T cells promotes increased immunopathology following Leishmania major infection. *PLoS Pathog*. **10**, e1003970 (2014).
17. Crosby, E.J., Clark, M., Novais, F.O., Wherry, E.J. & Scott, P. Lymphocytic Choriomeningitis Virus Expands a Population of NKG2D+CD8+ T Cells That Exacerbates Disease in Mice Coinfected with Leishmania major. *J Immunol*. **195**, 3301-3310 (2015).
18. Huang, C.H. et al. Innate-like bystander-activated CD38(+) HLA-DR(+) CD8(+) T cells play a pathogenic role in patients with chronic hepatitis C. *Hepatology*. **76**, 803-818 (2022).
19. Seo, I.H. et al. IL-15 enhances CCR5-mediated migration of memory CD8(+) T cells by upregulating CCR5 expression in the absence of TCR stimulation. *Cell Rep*. **36**, 109438 (2021).
20. Jeong, S. et al. IFITM3 Is Upregulated Characteristically in IL-15-Mediated Bystander-Activated CD8(+) T Cells during Influenza Infection. *J Immunol*. **208**, 1901-1911 (2022).
21. Lewis, R.S. Calcium signaling mechanisms in T lymphocytes. *Annu Rev Immunol*. **19**, 497-521 (2001).
22. Chatila, T., Silverman, L., Miller, R. & Geha, R. Mechanisms of T cell activation by the calcium ionophore ionomycin. *J Immunol*. **143**, 1283-1289 (1989).
23. Sun, L.J., Peterson B.R. & Verdine G.L. Dual role of the nuclear factor of activated T cells insert region in DNA recognition and cooperative contacts to activator protein 1. *Proceedings of the National Academy of Sciences*. **94**, 4919-4924 (1997).
24. Lodolce, J.P. et al. IL-15 receptor maintains lymphoid homeostasis by supporting lymphocyte homing and proliferation. *Immunity*. **9**, 669-676 (1998).
25. Kennedy, M.K. et al. Reversible defects in natural killer and memory CD8 T cell lineages in interleukin 15-deficient mice. *J Exp Med*. **191**, 771-780 (2000).
26. Becker, T.C. et al. Interleukin 15 is required for proliferative renewal of virus-specific memory CD8 T cells. *J Exp Med*. **195**, 1541-1548 (2002).

63 27. Goldrath, A.W. et al. Cytokine requirements for acute and Basal homeostatic
64 proliferation of naive and memory CD8+ T cells. *J Exp Med*. **195**, 1515-1522 (2002).
65 28. Geginat, J., Lanzavecchia, A. & Sallusto, F. Proliferation and differentiation potential of
66 human CD8+ memory T-cell subsets in response to antigen or homeostatic cytokines.
67 *Blood*. **101**, 4260-4266 (2003).
68 29. Correia, M.P. et al. Hepatocytes and IL-15: a favorable microenvironment for T cell
69 survival and CD8+ T cell differentiation. *J Immunol*. **182**, 6149-6159 (2009).
70 30. Correia, M.P., Costa, A.V., Uhrberg, M., Cardoso, E.M. & Arosa, F.A. IL-15 induces CD8+ T
71 cells to acquire functional NK receptors capable of modulating cytotoxicity and cytokine
72 secretion. *Immunobiology*. **216**, 604-612 (2011).
73 31. Liu, K., Catalfamo, M., Li, Y., Henkart, P.A. & Weng, N.P. IL-15 mimics T cell receptor
74 crosslinking in the induction of cellular proliferation, gene expression, and cytotoxicity in
75 CD8+ memory T cells. *Proc Natl Acad Sci U S A*. **99**, 6192-6197 (2002).
76 32. Balin, S.J. et al. Human antimicrobial cytotoxic T lymphocytes, defined by NK receptors
77 and antimicrobial proteins, kill intracellular bacteria. *Sci Immunol*. **3** (2018).
78 33. Seok, J. et al. A virtual memory CD8(+) T cell-originated subset causes alopecia areata
79 through innate-like cytotoxicity. *Nat Immunol*. **24**, 1308-1317 (2023).
80 34. Jabri, B. & Abadie, V. IL-15 functions as a danger signal to regulate tissue-resident T cells
81 and tissue destruction. *Nat Rev Immunol*. **15**, 771-783 (2015).
82 35. Ma, S., Caligiuri, M.A. & Yu, J. Harnessing IL-15 signaling to potentiate NK cell-mediated
83 cancer immunotherapy. *Trends Immunol*. **43**, 833-847 (2022).
84 36. Mishra, A., Sullivan, L. & Caligiuri, M.A. Molecular pathways: interleukin-15 signaling in
85 health and in cancer. *Clin Cancer Res*. **20**, 2044-2050 (2014).
86 37. Smith-Garvin, J.E., Koretzky, G.A. & Jordan, M.S. T cell activation. *Annu Rev Immunol*. **27**,
87 591-619 (2009).
88 38. Roberts, A.I. et al. NKG2D receptors induced by IL-15 costimulate CD28-negative effector
89 CTL in the tissue microenvironment. *J Immunol*. **167**, 5527-5530 (2001).
90 39. Deshpande, P. et al. IL-7- and IL-15-mediated TCR sensitization enables T cell responses
91 to self-antigens. *J Immunol*. **190**, 1416-1423 (2013).
92 40. Richer, M.J. et al. Inflammatory IL-15 is required for optimal memory T cell responses. *J*
93 *Clin Invest*. **125**, 3477-3490 (2015).

41. Vaeth, M., Kahlfuss, S. & Feske, S. CRAC Channels and Calcium Signaling in T Cell-Mediated Immunity. *Trends Immunol*. **41**, 878-901 (2020).
42. Clipstone, N.A. & Crabtree, G.R. Identification of calcineurin as a key signalling enzyme in T-lymphocyte activation. *Nature*. **357**, 695-697 (1992).
43. Azzi, J.R., Sayegh, M.H. & Mallat, S.G. Calcineurin inhibitors: 40 years later, can't live without. *J Immunol*. **191**, 5785-5791 (2013).
44. Lee, H.G. et al. Pathogenic function of bystander-activated memory-like CD4(+) T cells in autoimmune encephalomyelitis. *Nat Commun*. **10**, 709 (2019).
45. Langmead, B. & Salzberg, S.L. Fast gapped-read alignment with Bowtie 2. *Nat Methods*. **9**, 357-359 (2012).
46. Love, M.I., Huber, W. & Anders, S. Moderated estimation of fold change and dispersion for RNA-seq data with DESeq2. *Genome Biol*. **15**, 550 (2014).
47. Ritchie, M.E. et al. limma powers differential expression analyses for RNA-sequencing and microarray studies. *Nucleic Acids Res*. **43**, e47 (2015).
48. Stuart, T. et al. Comprehensive Integration of Single-Cell Data. *Cell*. **177**, 1888-1902 e1821 (2019).
49. Durinck, S., Spellman, P.T., Birney, E. & Huber, W. Mapping identifiers for the integration of genomic datasets with the R/Bioconductor package biomaRt. *Nat Protoc*. **4**, 1184-1191 (2009).